THE ASTRONOMICAL JOURNAL VOLUME 89, NUMBER 11 NOVEMBER 1984

RADIO AND OPTICAL MORPHOLOGY OF LOW-REDSHIFT QUASARS

ANN C. GOWER
Department of Physics, University of Victoria, Victoria, British Columbia, V8W 2Y2 Canada

J. B. HUTCHINGS
Dominion Astrophysical Observatory, Herzberg Institute of Astrophysics, Victoria, British Columbia, V8X 4M6 Canada
Received 10 January 1984; revised 24 July 1984

ABSTRACT

Snapshot VLA* radio maps are presented of a representative sample of low-redshift quasars, and radio properties summarized for 40 objects. Resolutions are typically 1.4″ at 20 cm and 0.4″ at 6 cm wavelength. Half the sources have a bright core and two lobes, while 20% have a single lobe. With data of dynamic range ~100, 55% have connecting luminous bridges between components, and more than half of these are curved. 25% of the sources are significantly nonlinear, and over 40% have cores with resolved structure. 20% of the sources are unresolved. Optical imaging data, principally from Hutchings, Crampton, and Campbell (1983), exist for 24 of the quasars. We discuss possible correlations between optical and radio morphology. Connections may exist between the core spectral index, the core radio luminosity, and optical nuclear luminosity. We also discuss orientations of radio and optical axes, and connections between radio size and structure and optical interactions.

I. INTRODUCTION

The radio morphology of quasars can be studied at arcsecond resolution with the VLA and in appropriate cases at milliarcsecond resolution with VLBI observations. Recent results have shown these to have a great variety, particularly in low-redshift objects ($z < 0.3$), where kiloparsec-sized structure can be mapped. At the same time, optical data of approximately the VLA resolution have been obtained of the host galaxies of many low-redshift QSOs. These separate studies have led to much discussion and speculation and, in particular, have drawn attention to the morphological similarities between quasars and galaxies, both optical and radio.

In this work, we discuss VLA data of a sample of 40 radio quasars of low redshift, and we are able to compare the radio and optical morphology of more than half of them, for the most part from our own data. In addition to the discussion of the new radio data and statistics, therefore, we are able to note a number of interesting connections wtih optical properties which may relate to our understanding of the active nucleus itself.

The radio morphology in general consists of a compact (< 0.4″ structure) flat-spectrum core coincident with the optical QSO, and extended structure of steeper spectral index which is typically double lobed, but may also consist of one or two jets or bridges, bent or straight, connecting the core and lobes. The relative fluxes of all components show great variation between objects and, in some cases, the lobes themselves have complex structure which may be regarded as a tracer of earlier, different jet orientations. The optical data (see, e.g., Hutchings, Crampton, and Campbell 1984; HCC) generally reveal the nature of the underlying galaxy, sometimes with distinct spiral characteristics, sometimes filaments or a halo outside the galaxy, and quite frequently a smaller galaxy apparently interacting with the QSO galaxy. In this paper, we study the correlations between the optical and radio morphologies of these objects.

The optical properties of the QSOs are discussed in full detail in HCC and Hutchings *et al.* (1984). The reader is referred to them for discussions on axial ratios, scale lengths, directions of optical axes, nuclear and fuzz luminosities, and morphological classifications. In our diagrams, we have chosen to show the optical and radio maps on the same scale. Hutchings *et al.* (1984) give the full optical maps for all sources. We also refer the reader to these papers for discussions on the meaning or otherwise of the designations QSO and Seyfert 1. The present sample are all in the QSO catalogue of Hewitt and Burbidge (1980: HB), with the exception of the 4 C08.66 objects, which have been classified by Harris *et al.* (1983). The sample is well distributed in optical luminosity and redshift, although most of them qualify as "genuine" optical QSOs, with M_V ($H_0 = 50$) < -23. We have used the positions given by HB for most optical objects. In cases where there appeared to be a discrepancy between our radio positions and these optical positions, we remeasured the optical positions on POSS prints. Comments are given in the text wherever this was done. Our optical positions are estimated to be good to 5″. Hintzen and Owen (1981) claim 0.5″ accuracy for optical positions of some of our objects, some of which disagree with Hewitt and Burbidge. These two are pointed out in the text.

The radio sources observed were principally selected to be a representative set of quasars from HB of redshift 0.3 or less, accessible from the VLA (i.e., north of ~ −25°). A few of the sources were not observed because of scheduling constraints, and a few sources of redshift a little larger than 0.3 were observed, because the optical structure was known. Thus while the sample is not complete or totally unbiased, we consider that it is reasonably representative of low-redshift quasars as a group.

Some of the sources were reported by Hutchings *et al.* (1982: paper 1). They are included in this paper as they form part of the sample. We have not, in general, tried to include in the discussion quasars for which we do not have our own data, in order to keep the data set and measures as uniform as possible. For this reason, 3C 273 and 3C 206 are not included. We have made use of comparable VLA data by other authors on three quasars for which we have optical data (Harris *et al.* 1983; Neff 1982), and we refer to one optical image by Wyckoff, Wehinger, and Gehren (1981: WWG). A few other radio quantities are taken from the literature for

*The VLA is a facility of the NRAO, which is operated by Associated Universities Inc. under contract with the NSF.

 0004-6256/84/111658-30$00.90

the largest sources. Several objects have also been observed at 20 cm by Hintzen, Ulvestad, and Owen (1983: HUO).

II. OBSERVATIONS AND MAPS

All new snapshot observations were made in the A configuration of the VLA, in April 1982, generally at both 6- and 20-cm wavelengths, with two 10-min scans on each object, separated by about 2 hr in hour angle. The resulting maps were cleaned and, where possible, were self-calibrated to obtain higher dynamic range. Our limiting flux is ~1 mJy and our dynamic range is ~100, with extremes of 50 and 1000. Table I lists various selected properties for all the sources, and in Fig. 1 we show the maps for all well-resolved sources where our data add appreciably to the detailed knowledge of the source structure. Table II gives the contour levels and peak fluxes for all maps. Where available, we also show as an inset the optical maps on the same scale. Full versions of the optical data are published elsewhere (Hutchings *et al.* 1984).

These quasars show a wide variety of radio structures, and care should be taken in interpreting the maps, since some flux may be missing from the larger-scale structures. The smallest spacing of the VLA in the A configuration is 1 km and the largest-scale structure visible in these observations is

TABLE I. Quasar data and measures ($H_0 = 100$, $q_0 = 0$).

Object Name		z	Radio Properties: Core flux(mJy) 20cm	6cm	α (core)	log(Lcore) 6cm (W/Hz)	Lobe Peak distances(Kpc)		Size (Kpc)	Type[a] (+angle)	Optical Properties: M_N	M_G	Morphology[b]	Other Radio Maps[d]
0007+106	III Zw 2	0.09	340	470	0.27	24.61	-	-	-	C	-21.8	-20.9	S,G	
0017+257	4C 25.01	0.28	240	310	0.21	25.34	70	(75)	(140)	CLL,133°				1
0041+119	4C 11.06	0.23	11	17	0.36	23.91	43	(65)	108	LLC,W,171°				1
0100+108	MC 2	0.14	48	11	-1.22	(23.33)	-	-	3.3	LL?				1
			48	>8	-1.48	(23.22)								
0137+012	4C 01.04	0.26	230	150	-0.35	25.02	32	43	75	CLL,W	-	-	(I?,G)[c]	1,7
0241+622		0.04	160	300	0.52	23.70	2.0	-	2.0	CL	-23.1	-20.9	S	2
0736+017	0I+061	0.19	2190	2240	0.02	25.91	-	-	-	C				
0742+318[c]	4C 31.30	0.46	610	640	0.04	26.07	180	200	470	CLL	-25.5	-	I??	3
0829+047	0J+049	-	740	656	-0.10	-	-	-	-	C				
0846+100	4C 09.31	0.37	7	6	-0.13	23.90	86	120	210	LCL,167°	-21.5	-20.1	Ir,G,I?	4
0851+202	0J+287	0.31	2270	3200	0.29	26.78	-	-	-	C	-26.3	>-23.1	(-)	1
0952+097	4C 09.35	0.30	9	7	-0.21	23.80	12	25	38	LCL,165°,W				5
0957+227	4C 22.25	(0.1)	-	-	-	-	-	-	46	LL	-19.4	-18.2	I	4
1004+130	4C 13.41	0.24	20	12	-0.42	23.79	120[c]	(83)[c]	(250)[c]	CLL,170°[c]				
1011-282	0L-219	0.25	27	37	0.26	24.32	60	140	190	CLL,157°	-24.0	-21.5	H	
1020-103	0L-133	0.20	-	330	-	(25.12)	3.0	-	3.0	CL	-22.8	-19.5	(-)	
1028+313	0L+347	0.18	89	110	0.18	24.54	(9)	(28)	(50)	CLL,W				
1203+011	PKS	0.10	130	170	0.22	24.24	-	-	≤1	(C)	-19.5	-	I?,G,F	
1217+023	0N+029	0.24	220	320	0.34	25.22	(130)[c]	(125)[c]	(280)[c]	CLL,W				3
1223+252	4C 25.40	0.27	2.4	4.0	0.31	23.42	100	95	190	LLC				4
1243-072	0N-073	0.27	850	1300	0.35	25.93	8	9	27	CLL				
1254-333	PKS	0.19	-	-	-	-	-	-	53	LL,W	-20.4	-20.1	H	
1302-102	0P-106	0.29	570	1185	0.61	25.91	18	20	45	CLL,120°	-25.0	-23.6	H	
1400+162	4C 16.39	0.24	190	130	-0.32	24.89	(7.2)	(22)	(60)	CLL,130°,W	-22.8	-21.8	I?,G	5
1525+227	0R+241	0.25	43	43	0.0	24.42	13	-	13	CL	-23.0	-21.3	I?	
1545+210	3C 323.1	0.26	35	-	-	(24.36)	75	104	186	LLC,W				
1635+119	MC 2	0.15	16	17	0.05	23.58	126	-	126	CL	-21.2	-20.0	I?	
1721+343	4C 34.47	0.21	450	370	-0.20	25.22	240	264	>540[c]	CLL				9
1725+044	PKS	0.29	560	730	-0.16	25.78	12	-	12	CL	-21.7	-21.2	I?,G	
1739+184	4C 18.51	0.19	23	25	0.07	23.95	220	210	445	LLC,172°,W				1
2135-147	0X-158	0.20	87	126	0.31	24.67	140	180	260	LCL,W	-23.5	-22.2	I,G	
2141+175	0X+169	0.21	370	280	-0.23	25.10	-	-	-	C	-23.7	-22.2	S?,F	
2201+315	4C 31.63	0.30	1100	1500	0.26	26.08	110	120	230	CLL,165°,W	-24.5	-23.5	I?	3
2217+08N[c]	4C 08.66	0.62	22	27	0.17	24.91	55	70	120	CLL,138°	-21.7	-24.8	G	6
2217+08S[c]	4C 08.66	0.22	8	7	-0.11	23.53	120	130	250	CLL,W	-20.5	-22.3	(-)	6
2247+140	4C 14.82	0.24	(1870)	(1210)	(-0.36)	(25.80)	-	-	≤2	CL	-22.4	-21.5	(-)	
2305+187	4C 18.68	0.3	80	81	0.01	24.86	(5)	(13)	(24)	CLL,W	-22.3	-24.2	Ir,G,I?	1,8
2328+167	MC 3	0.28	-	25	-	(24.27)	2.2	-	2.2	CL?				
			-	13	-	(23.99)								
2331-240	0Z+252	0.05	-	910	-	(24.38)	-	-	-	C	-17.9	-18.8	(-)	
2355-082	PKS	0.21	-	110	-	(24.68)	2.7	-	2.7	CL				

All quantities in parentheses are uncertain due to diffuseness of lobes, unresolved structure, or assumed (α = 0) spectral lines.

[a] Core and Lobe(s) in (λ6cm) order of flux. W = wiggly connecting bridge. Bent sources have angles.

[b] From HCC : S = spiral, G = group, I = interaction, H = Halo, F = filament, Ir = Irregular

[c] Object or data from other sources. See notes for references.

[d] 1. Hintzen, Utvestad & Owen (1983 (20 cm VLA)
2. Hutchings et al. 1981 paper 1 (20, 6 cm VLA)
3. Neff 1982 (20, 6 cm VLA)
4. Miley & Hartsuijker 1978 (WSRT)
5. Hintzen & Owen 1981 (20 cm VLA)
6. Harris et al. 1983 (20, 6 cm VLA)
7. Gower & Hutchings 1982 (20, 6 cm VLA)
8. Gower & Hutchings 1984 (20, 6 cm VLA)
9. Jagers et al. 1980 (WSRT)

TABLE II. Radio contour levels and peak fluxes (all maps also have negative of lowest contour level).

Object	λ (cm)	Percent Levels of Peak 90	70	60	50	40	30	20	10	5	2	1	.5	.2	.1	Peak flux mJy/beam
0017+257	20	•	•		•	•	•	•	•	•	•	•	•	•		223
	6	•	•		•	•	•	•	•	•	•	•	•			306
0041+119	20	•	•		•	•	•	•	•	•	•	•	•	•		217
0100+108	20	•	•		•	•	•	•	•	•	•	•				48
0846+100	20	•	•		•	•	•	•	•	•	•					15
0952+097	6	•	•		•	•	•	•	•	•	•					14
0957+227	20	•	•		•	•	•	•	•	•	•	•				112
	6	•	•		•		•	•	•	•	•					29
1011−282	20	•	•		•		•	•	•	•	•					91
1020−103	6		•				•		•		•		•			334
1028+313	20	•	•		•	•	•	•	•	•	•	•				89
	6	•	•	•	•	•	•	•	•	•	•	•	•	•	•	105
1223+252	20	•	•		•	•	•	•	•	•	•					49
1243−072	20	•	•		•	•	•	•	•	•	•	•	•	•	•	845
1254−333	20	•	•		•		•	•	•	•	•	•	•			299
1302−102	20(T)	•	•		•	•	•	•	•	•	•	•	•			570
1400+162	20	•	•		•	•	•	•	•	•	•	•				191
	6	•	•		•	•	•	•	•	•	•	•				132
1525+227	20	•	•		•	•	•	•	•	•	•	•	•	•		219
	6	•	•		•	•	•	•	•	•	•	•	•	•		43
1545+210	20	•	•		•	•	•	•	•	•	•	•				298
1725+044	20	•	•		•	•	•	•	•	•	•	•	•	•	•	557
1739+184	20(T)	•	•		•	•	•	•	•	•	•					77
2135−147	20(T)	•	•		•	•	•	•	•	•	•					58
2201+315	20	•	•		•	•	•	•	•	•	•	•	•	•	•	1299
	20T	•	•		•	•	•	•	•	•	•	•	•	•		1315
2328+167	6	•	•		•	•	•	•	•	•	•	•				25
2355−082	6	•	•		•	•	•	•	•	•	•	•				64

35″ at 20 cm and 10″ at 6 cm. The maps are therefore only complete for structure of angular scale less than these scale sizes.

In Table I, we list, where possible, peak fluxes at 20 and 6 cm, and spectral index and luminosity at 6 cm, for the core components of these quasars. For the extended sources, we give the projected separations in kpc ($H_0 = 100$, $q_0 = 0$) of the lobe flux peaks from the quasar core, and also an estimate of the overall projected linear extent in kpc of the source (usually the sum of the above). In cases where the lobe maxima are diffuse, the numbers are given in parentheses. We also give a simple classification indicating the presence of core and lobe(s) in order of peak flux. In some cases, the relative flux levels reverse between 20- and 6-cm wavelengths: in these cases, the 6-cm levels are quoted. A few optical properties are listed for the objects with such data. For full details, see HCC or references therein.

Table I contains some sources or measures derived from other sources in order to fill out our radio/optical comparison. These are indicated with a footnote. We note that the quasar 0054 + 144 was not detected at the position given in HB. Three sources were marginally resolved at 20 cm and we do not quote core fluxes for them: 1020 − 103, 2328 + 167, and 2355 − 082. At 6 cm, they are resolved, but we do not always know which is the core component.

III. NOTES ON INDIVIDUAL SOURCES

We give below a brief commentary on most of the sources, together with reference to some other work on them. We also indicate, where possible, the flux missing in our 20-cm maps. The missing flux was estimated by noting the total power flux measurements for the sources, at the appropriate frequency, generally from the 1983 version of the Ohio radio-source listing. These numbers are intended to show to the nearest 10% how complete the VLA maps are.

In classifying these sources, we have chosen to use simple morphological descriptions, rather than terms which sometimes are taken to imply a physical process or property. Thus, if a structure is extended between its core and outer lobe, we note the presence of a filament or bridge (which may be a "jet"). Linear structure close to, and merged with, the core is referred to as a jet. The radio axis always refers to the line joining the core and lobe peaks. If the structure is significantly nonlinear, whatever its bending angle, we call it bent, and if an extended filament is not straight, we call it curved.

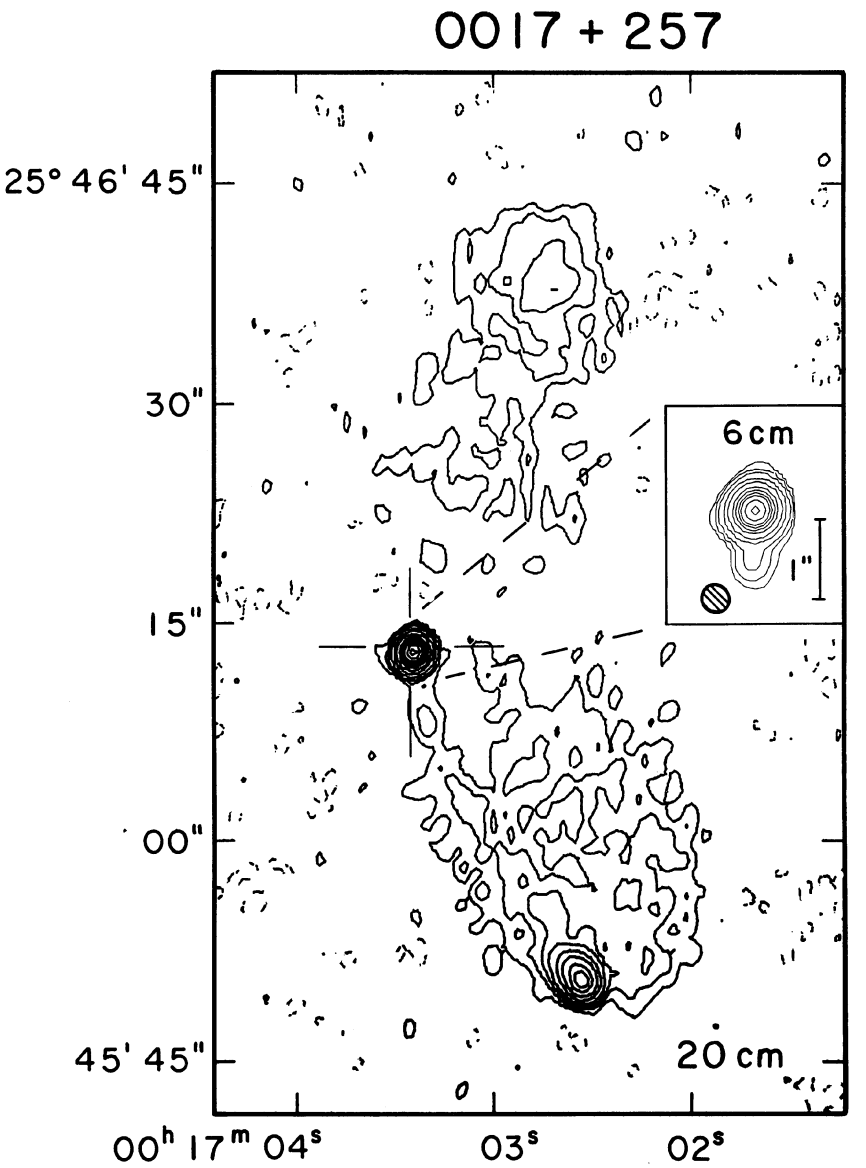

FIG. 1. Contour plots of VLA and optical maps. Radio contour levels are given in Table II. Optical maps are shown at the same scale as the (adjacent) radio map, and have levels a factor 2 apart (see Hutchings *et al.* 1984b). Crosses mark best optical positions, which are generally accurate to $\pm 2''$ or worse (see the text). In cases of disagreement between published values, we use those of HUO or Hintzen and Owen (1981). Where they lie close to the radio core, it is assumed that they coincide. Beam widths are indicated where significant. Optical beam widths are near 1". In 2355 − 082 we show polarization vectors.

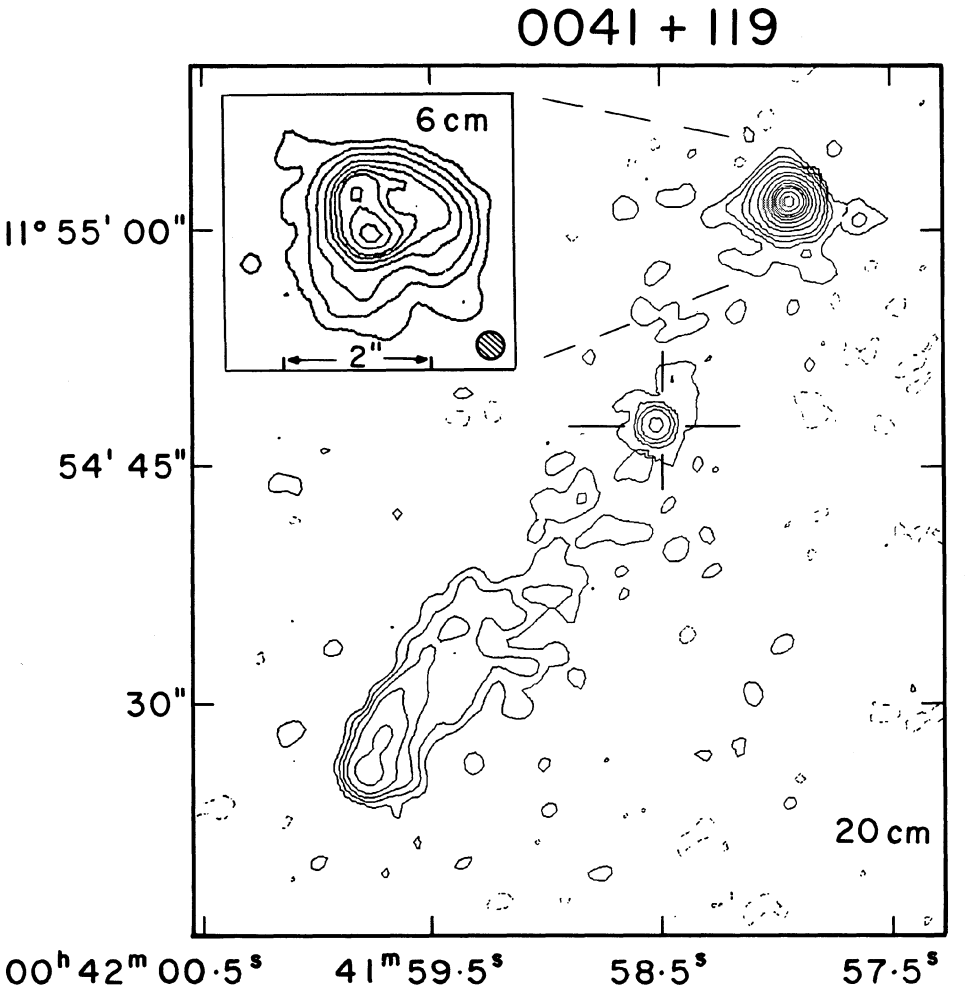

FIG. 1. (continued)

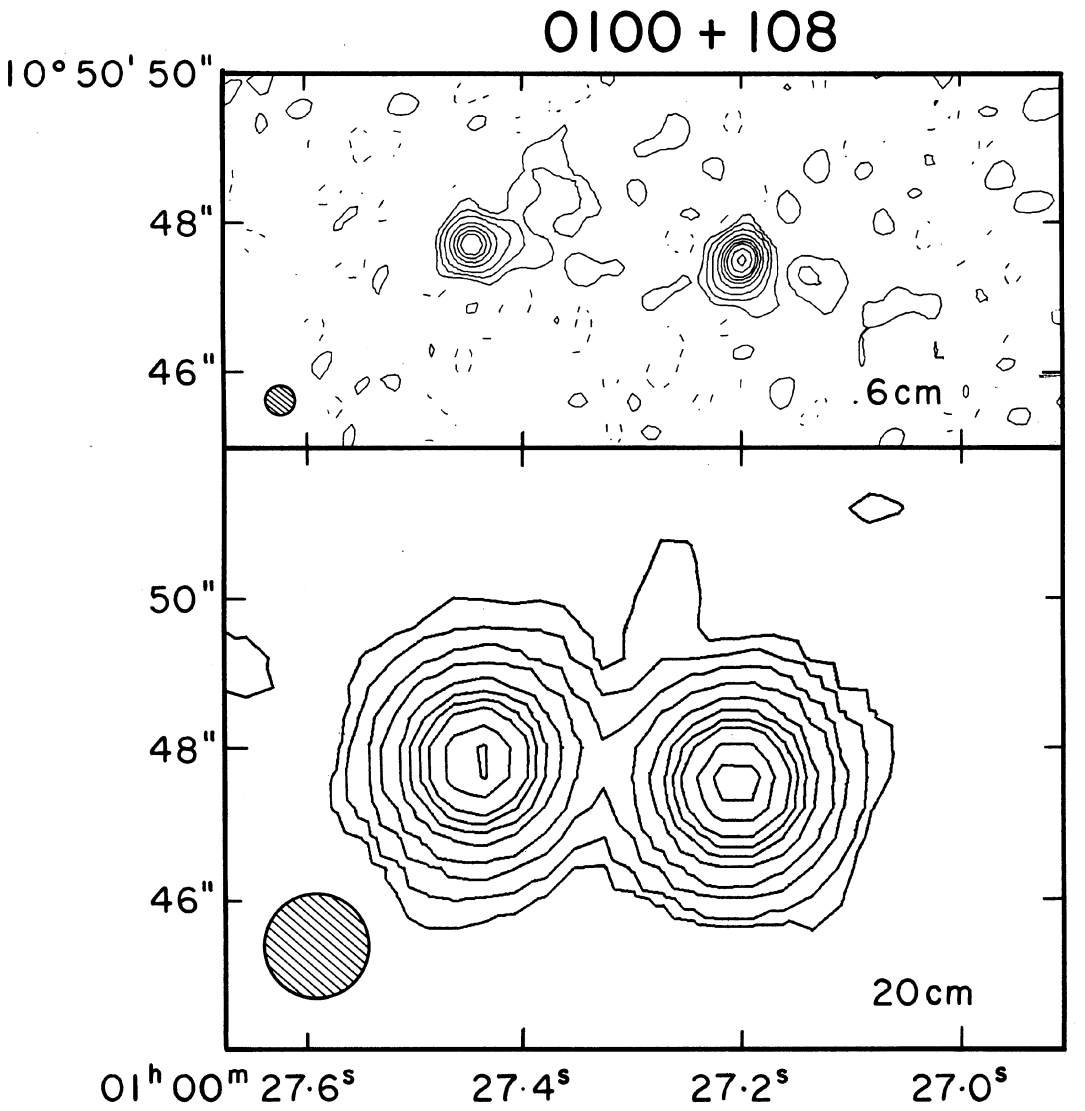

FIG. 1. (continued)

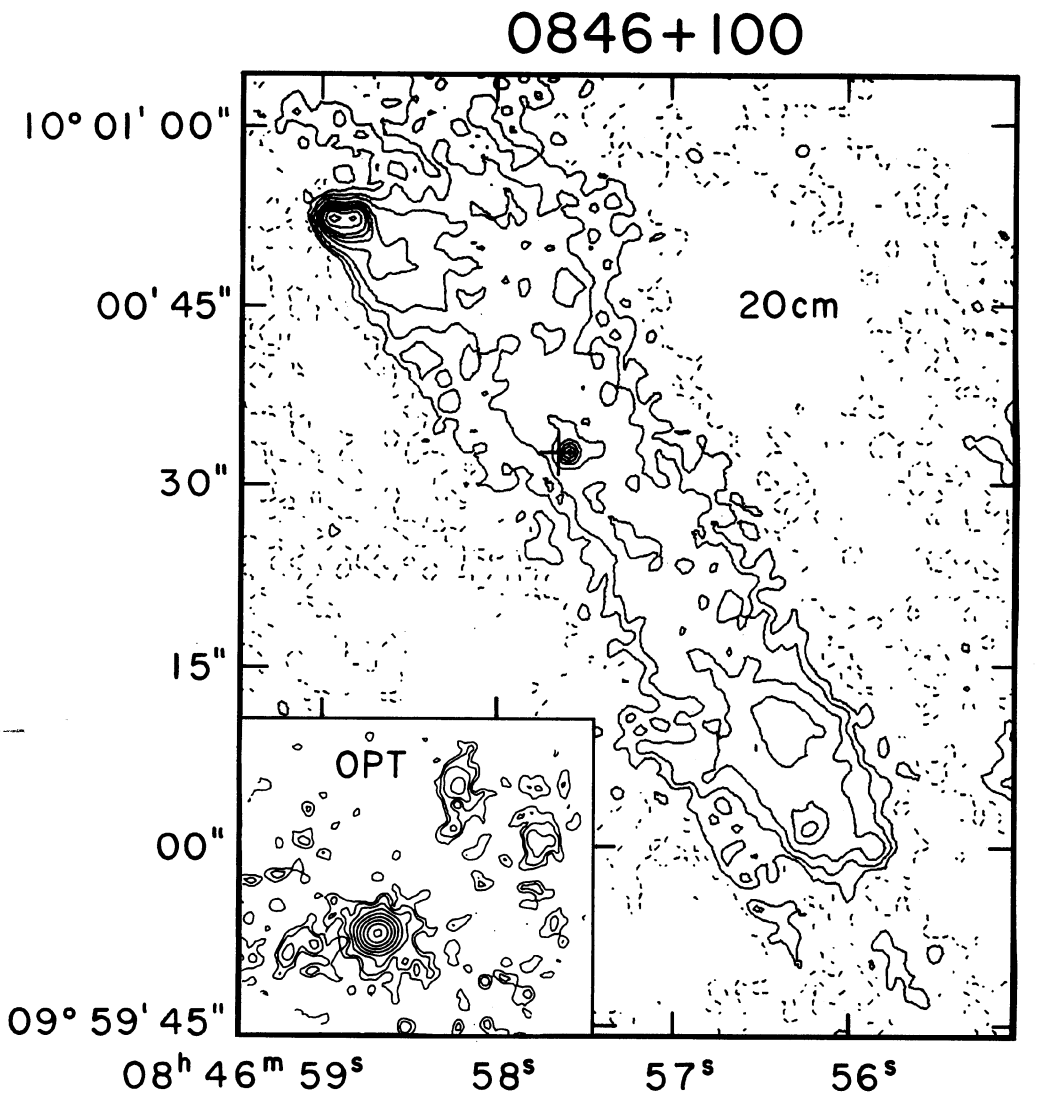

FIG. 1. (continued)

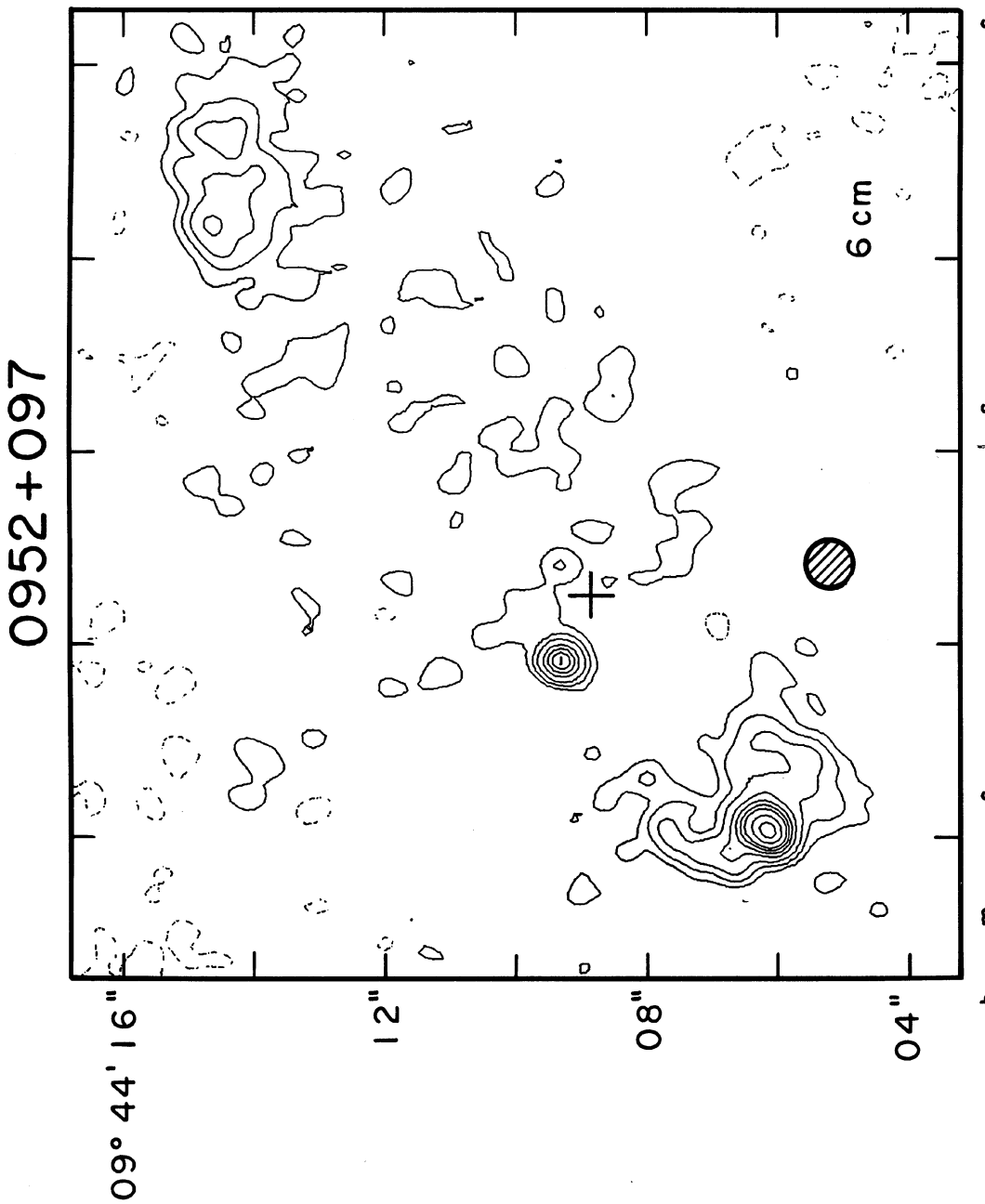

FIG. 1. (continued)

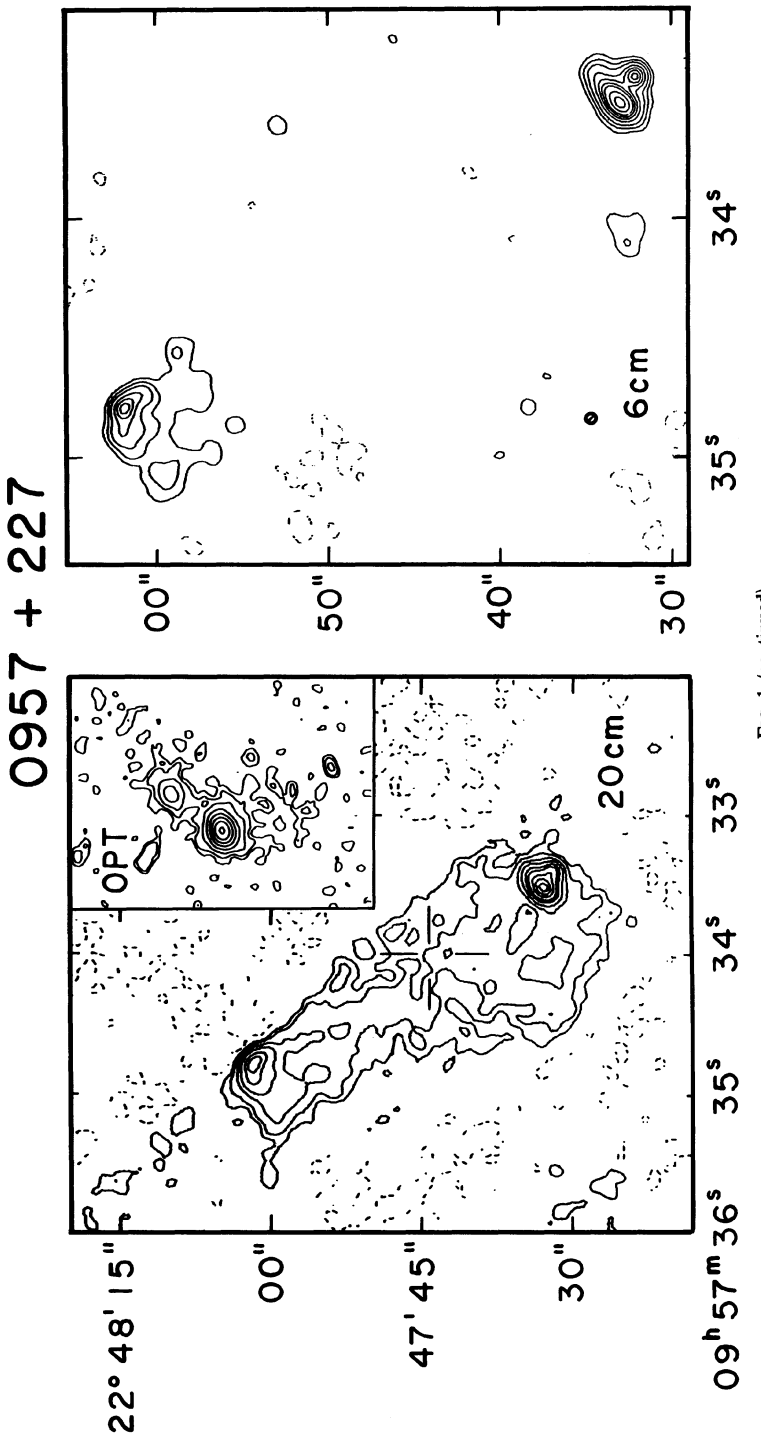

FIG. 1. (continued)

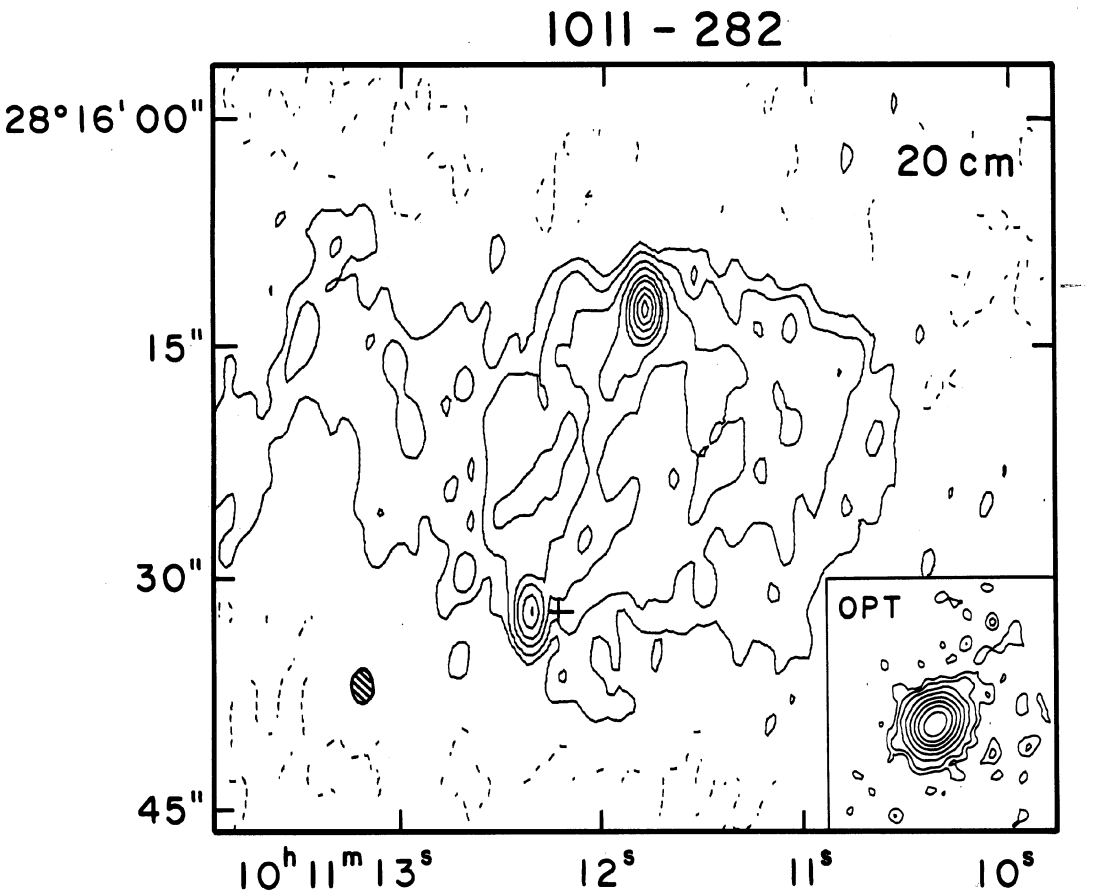

FIG. 1. (continued)

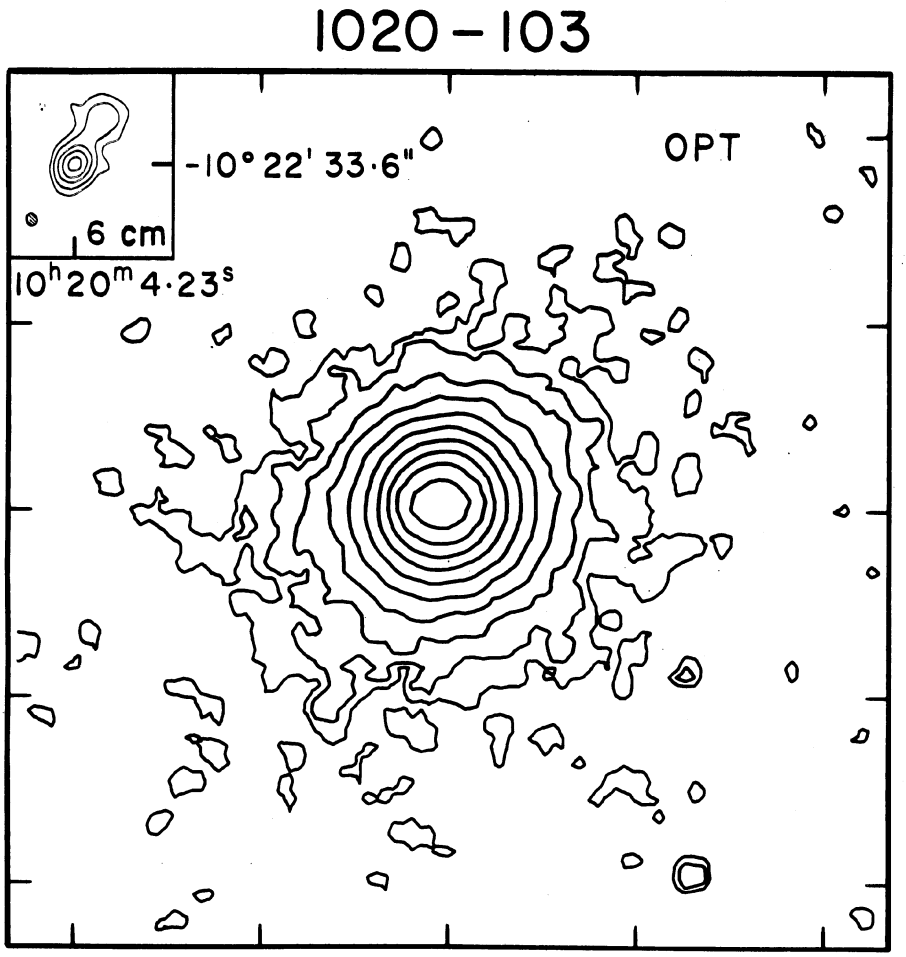

FIG. 1. (continued)

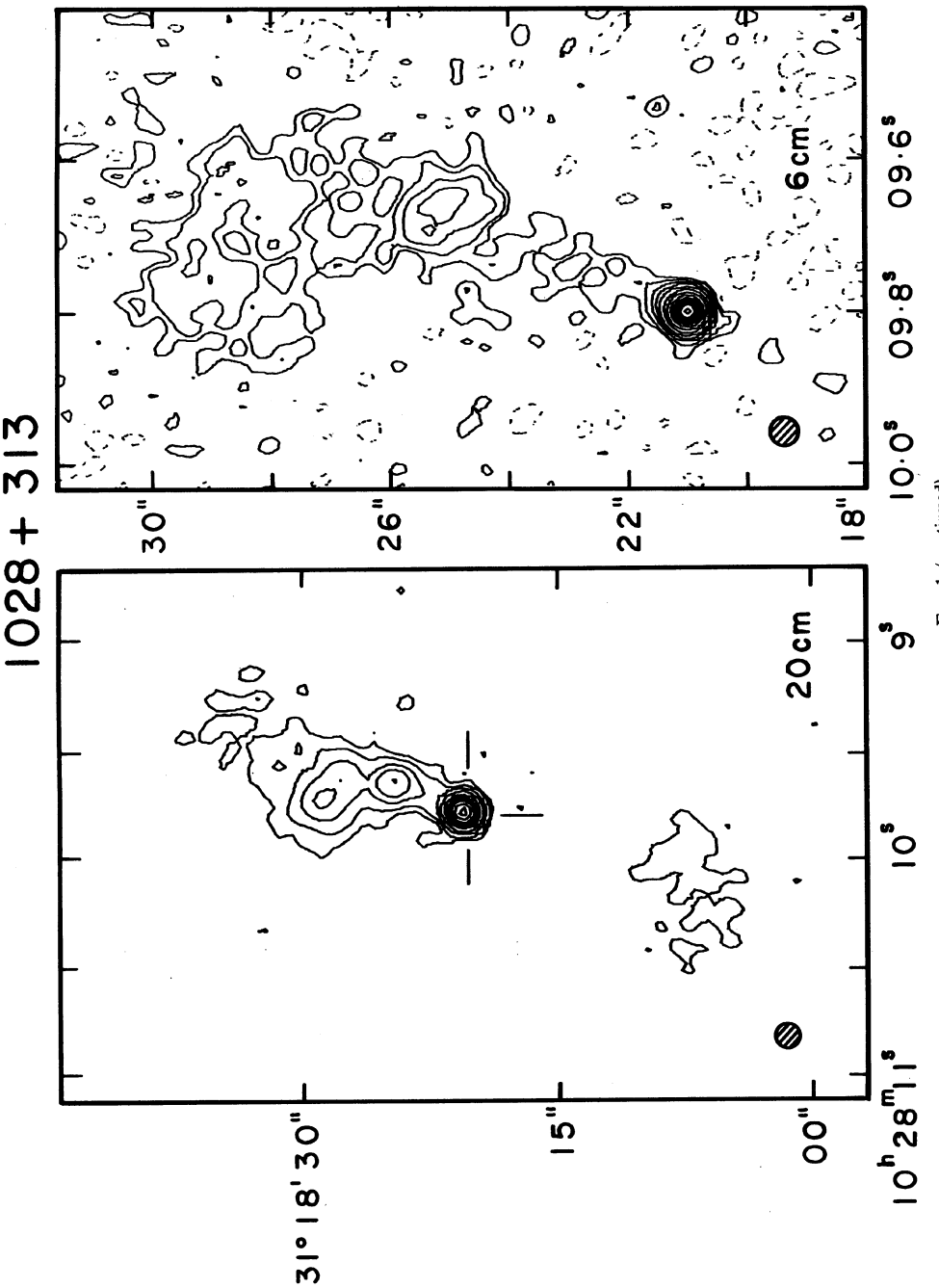

FIG. 1. (continued)

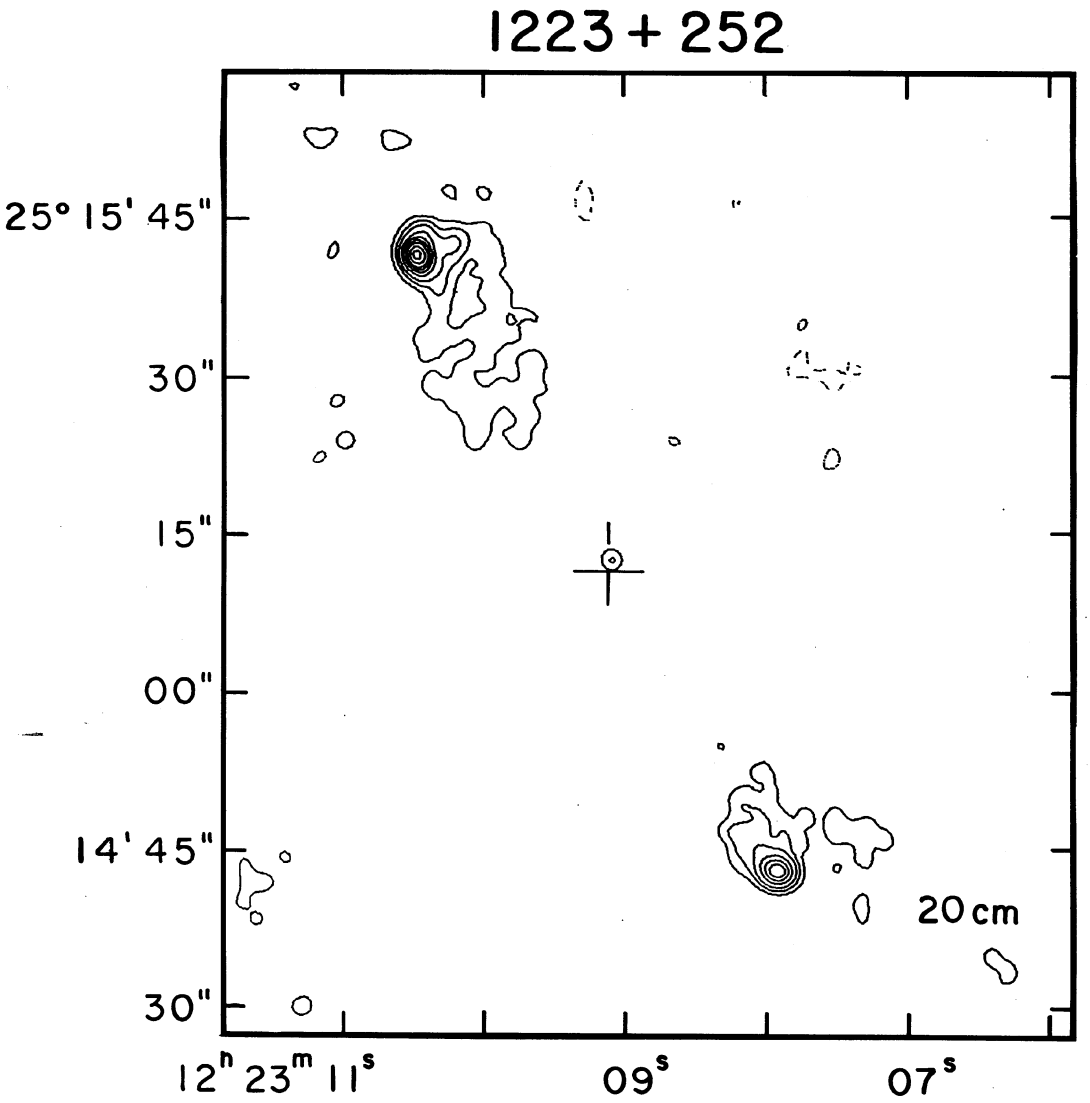

FIG. 1. (continued)

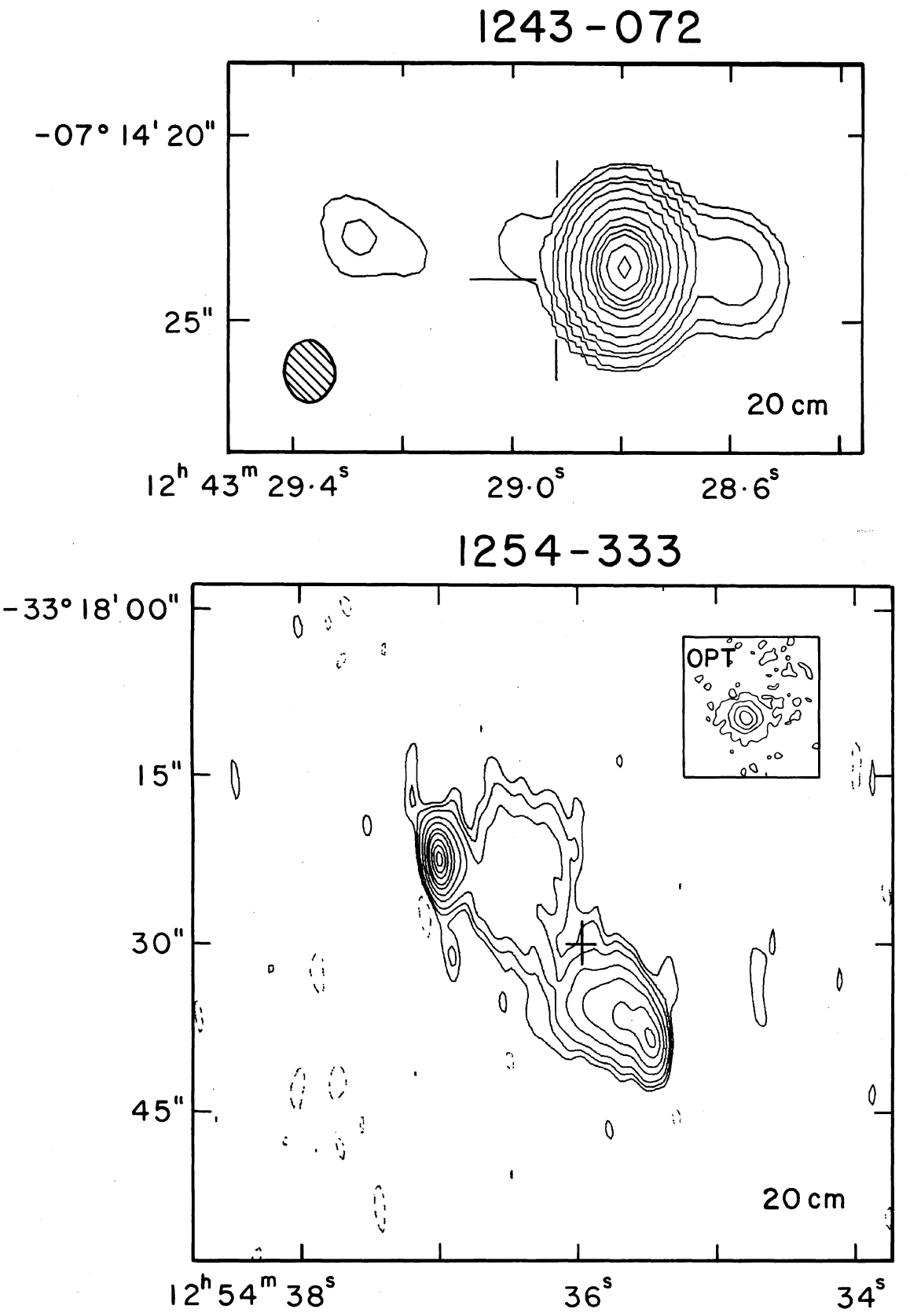

FIG. 1. (continued)

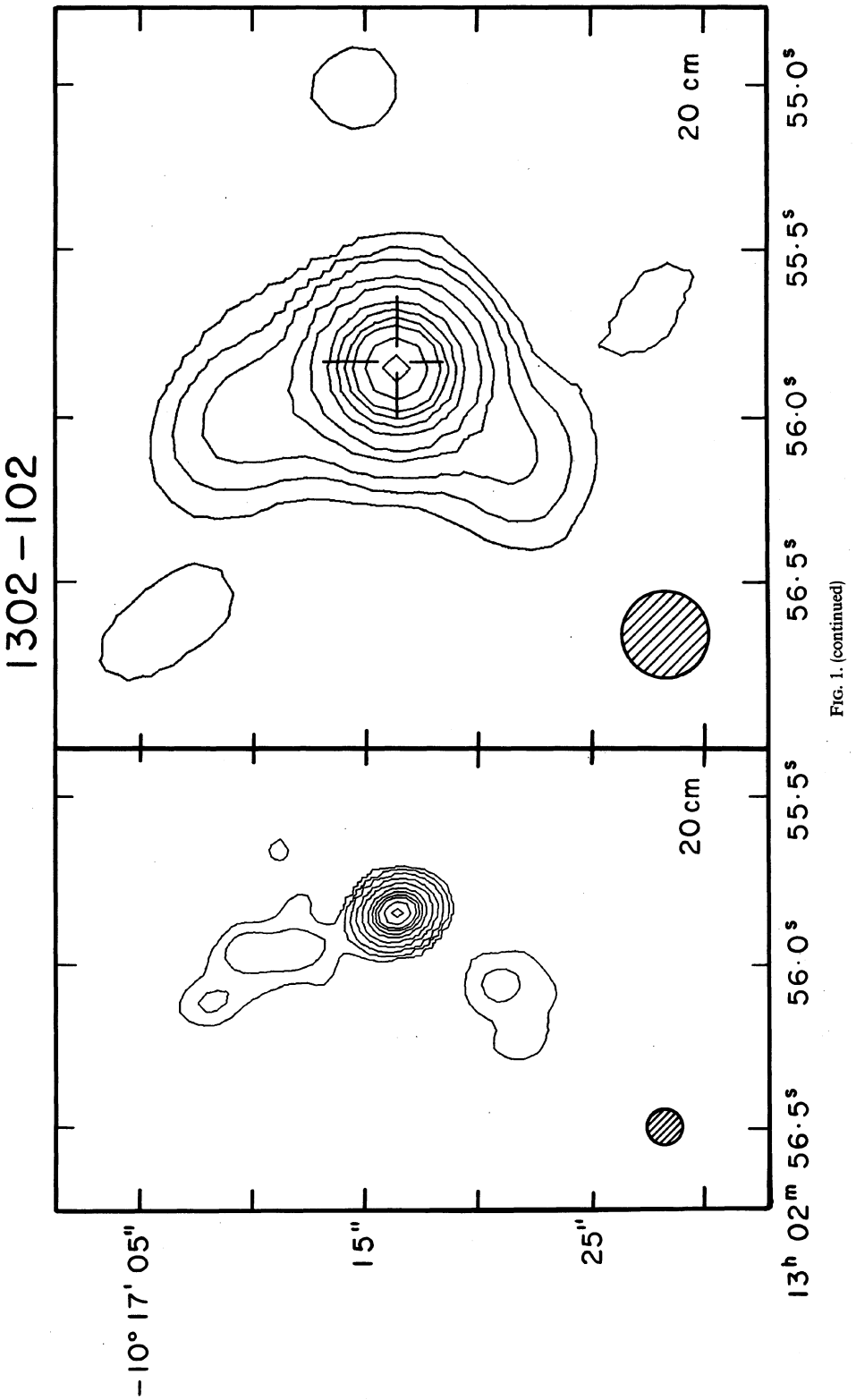

FIG. 1. (continued)

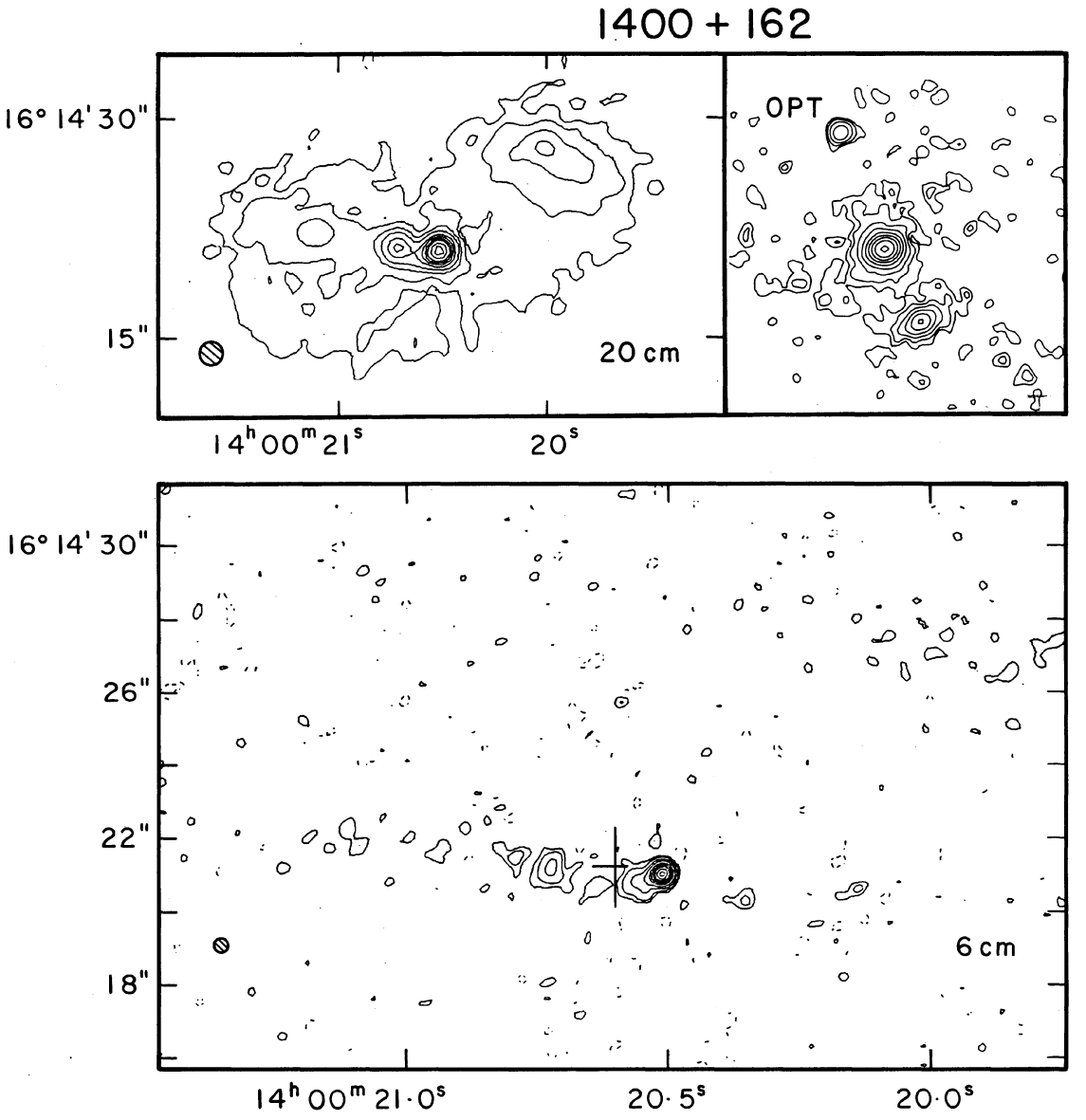

FIG. 1. (continued)

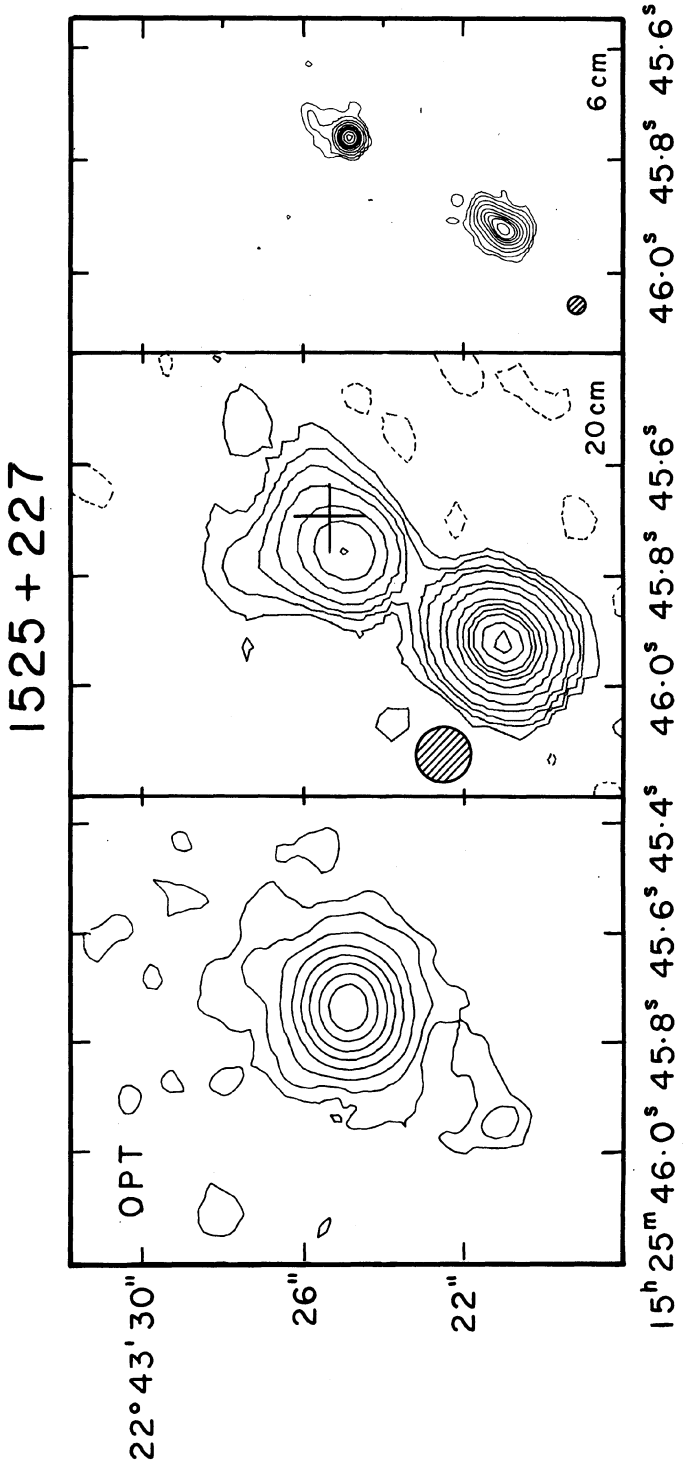

FIG. 1. (continued)

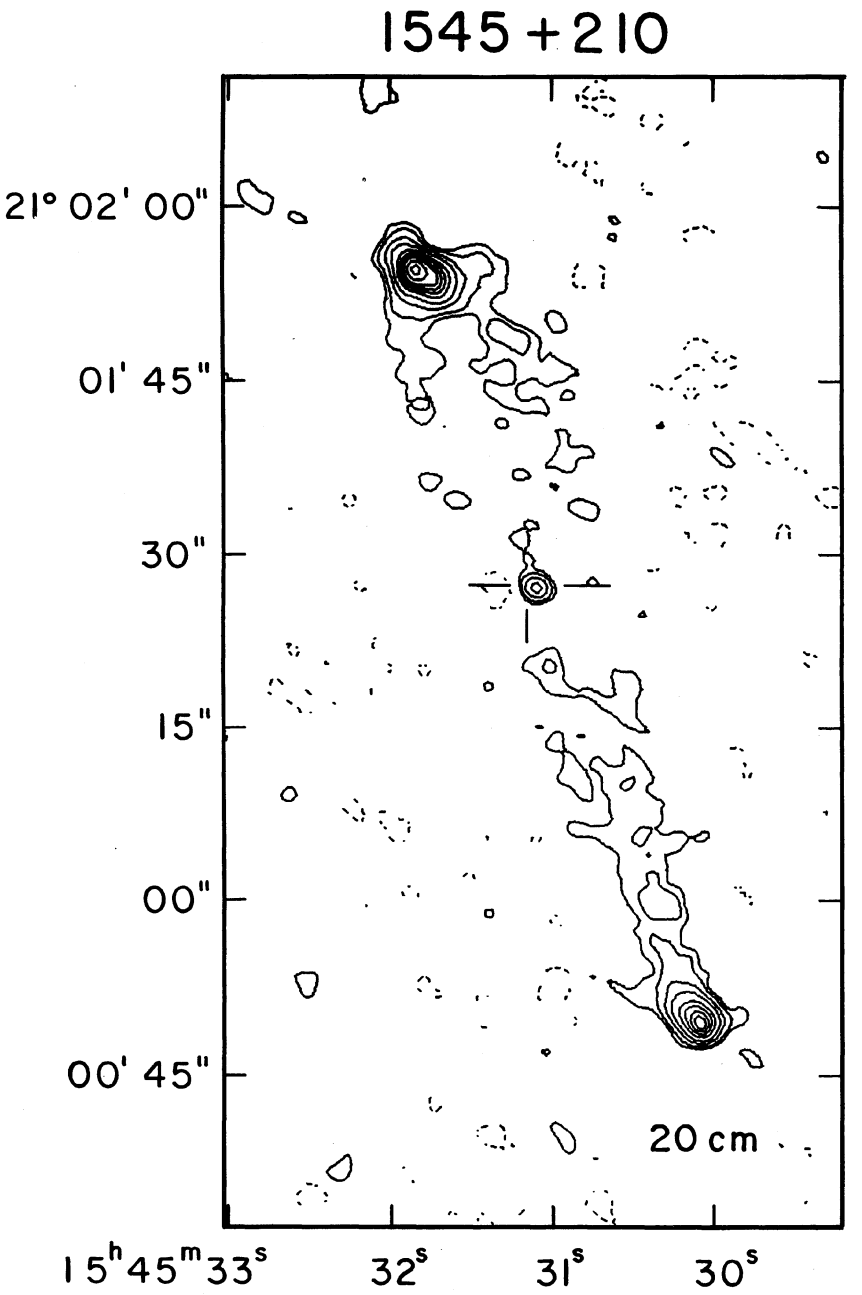

FIG. 1. (continued)

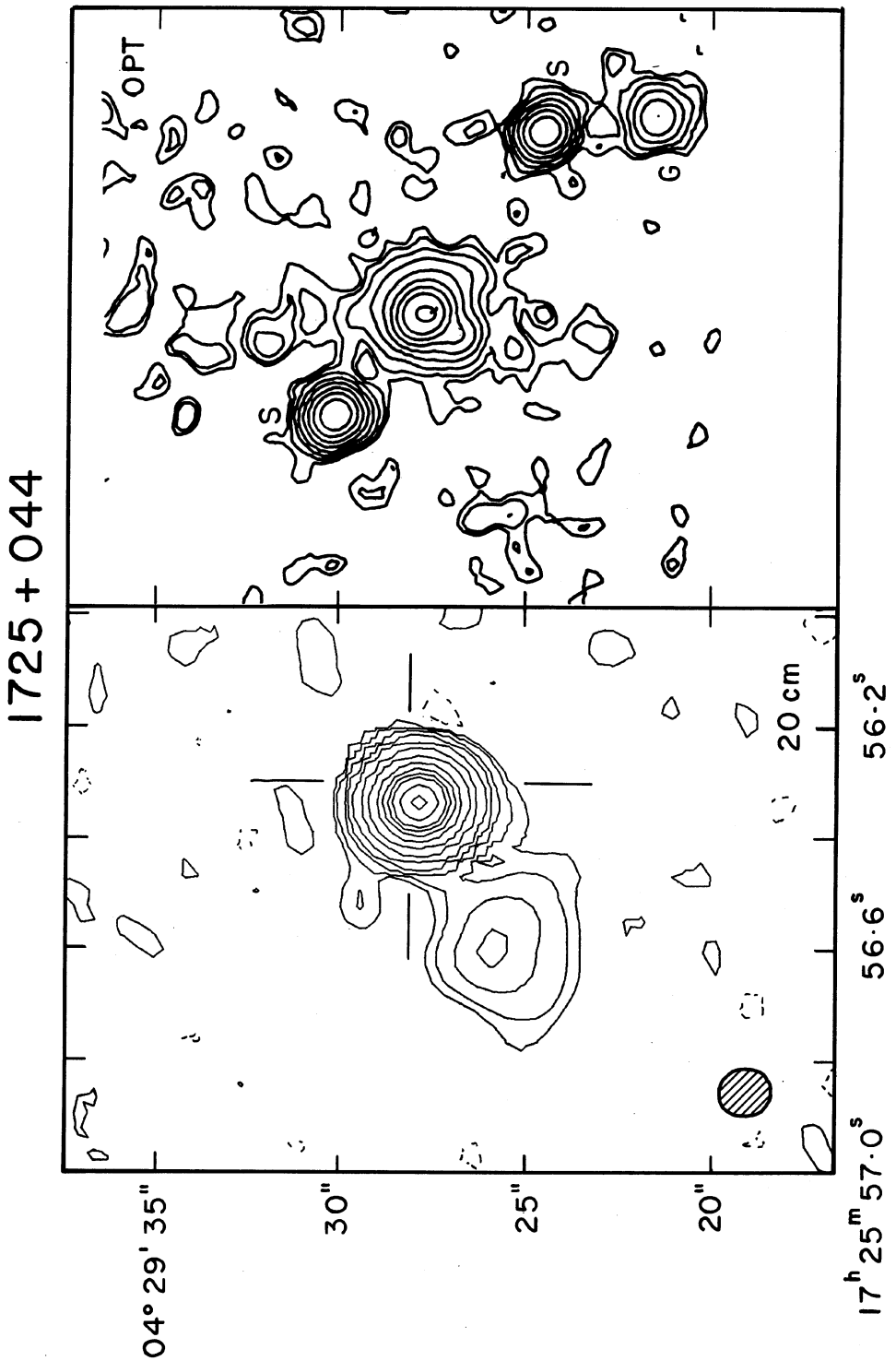

FIG. 1. (continued)

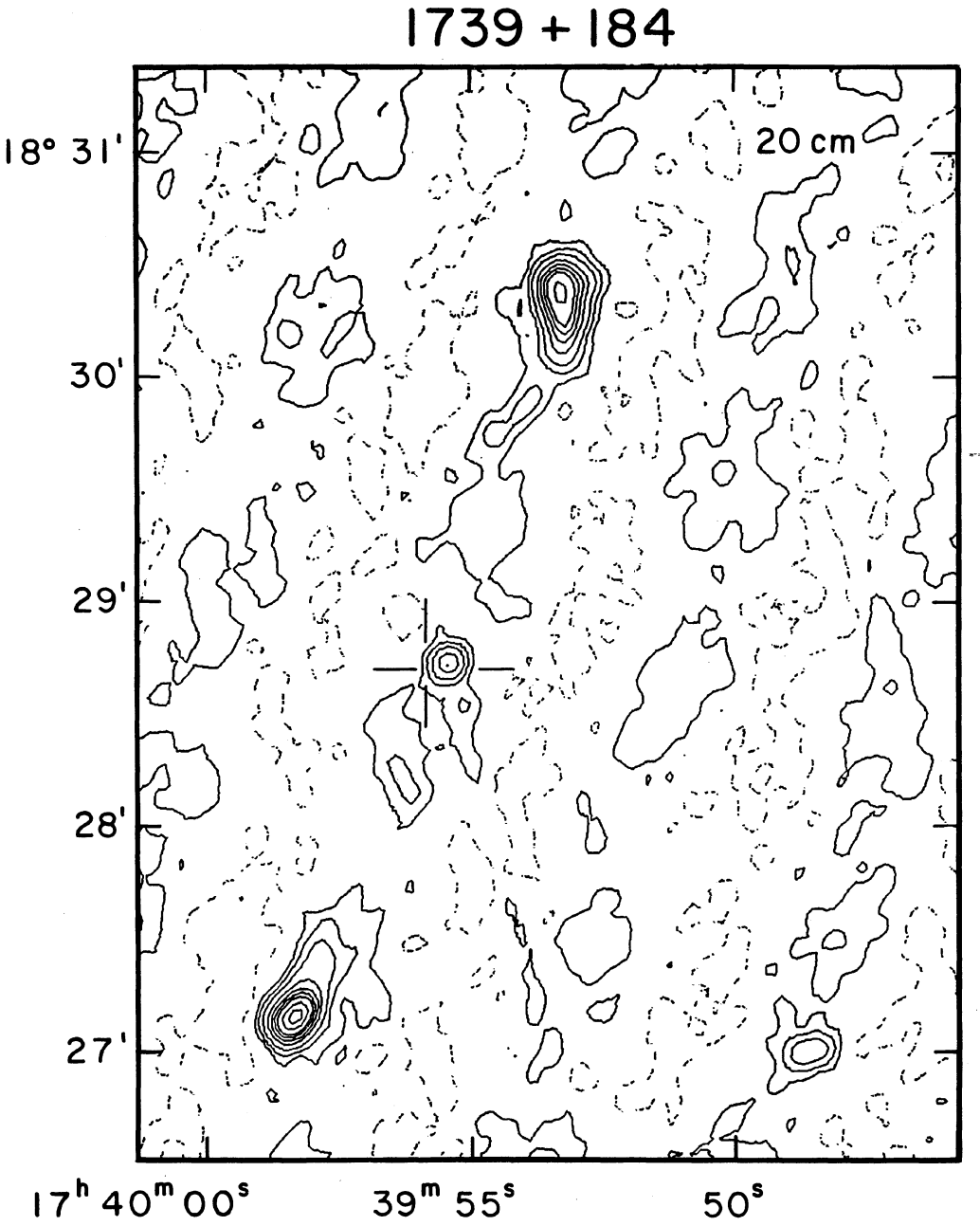

FIG. 1. (continued)

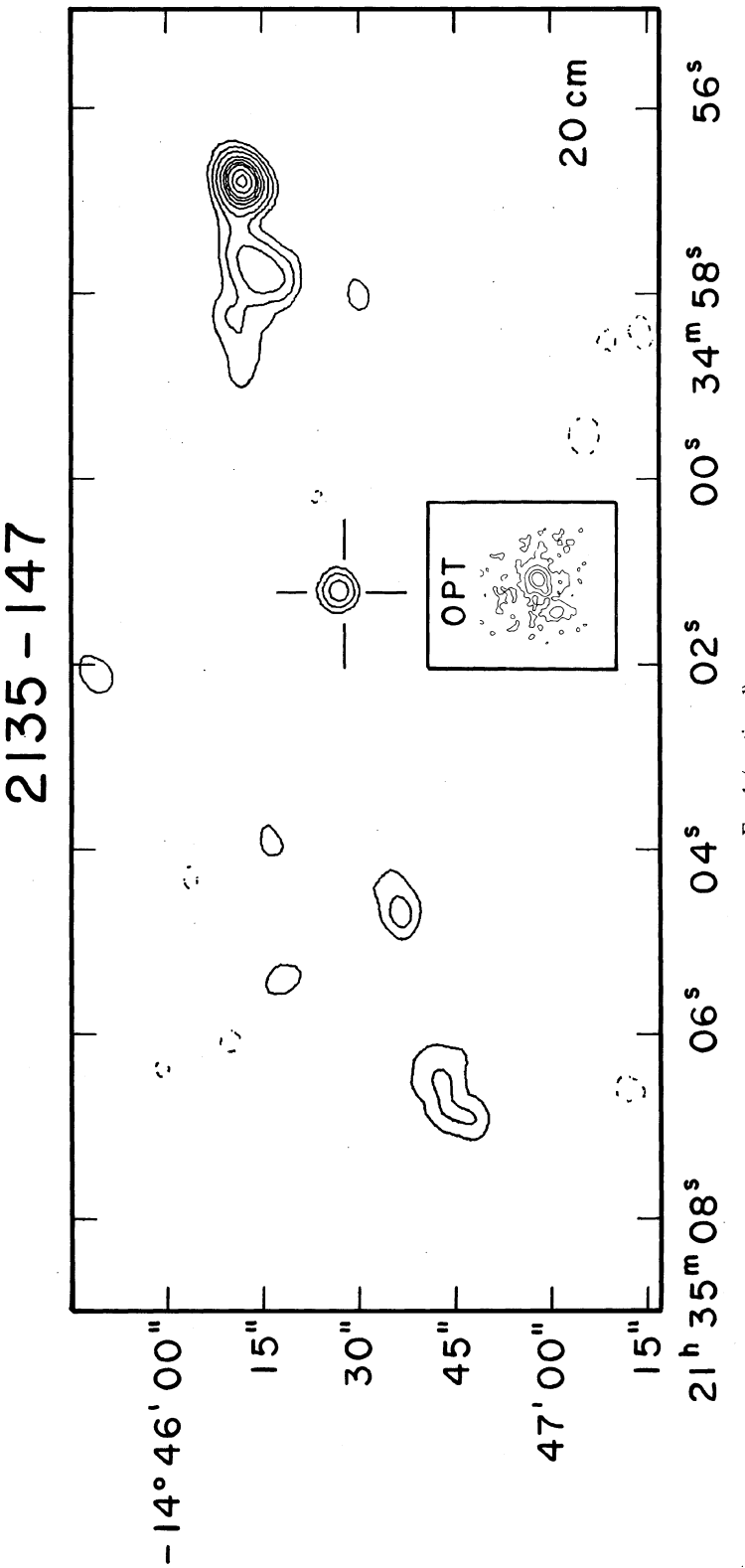

FIG. 1. (continued)

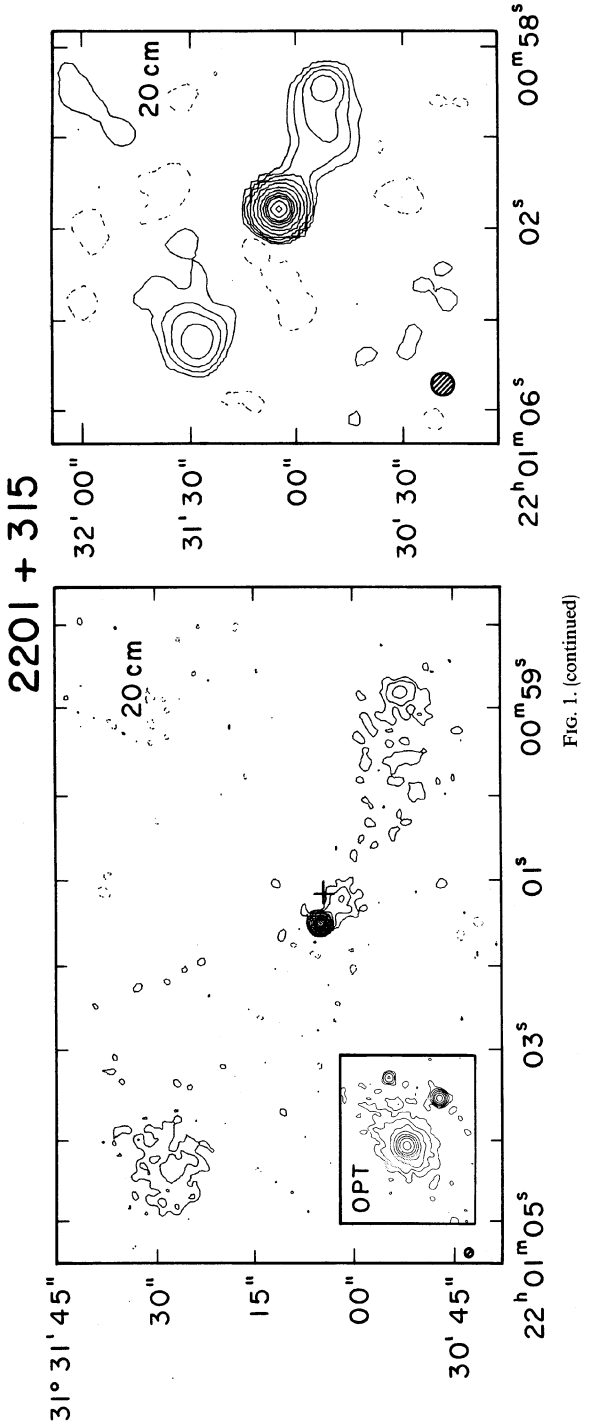

FIG. 1. (continued)

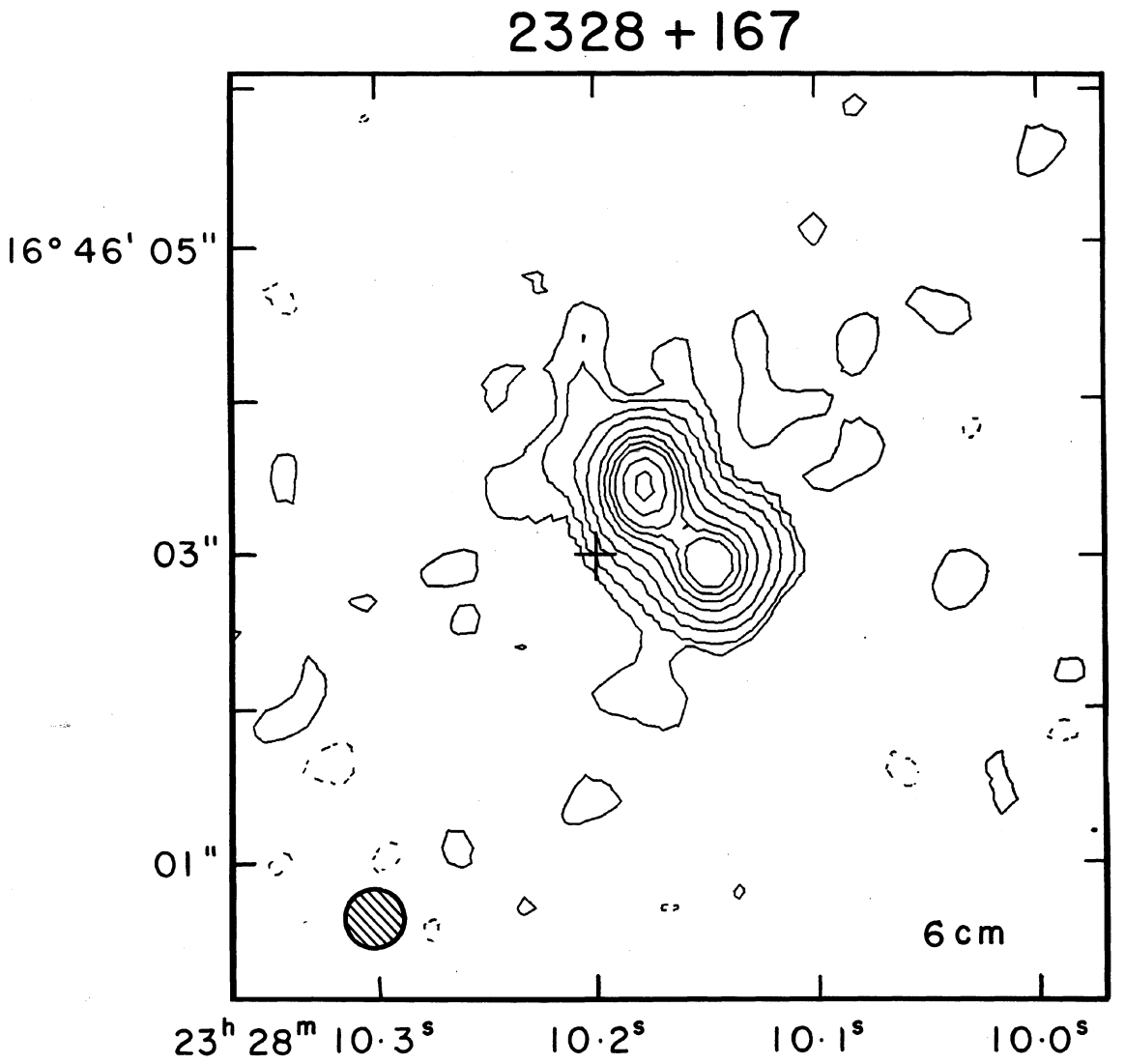

FIG. 1. (continued)

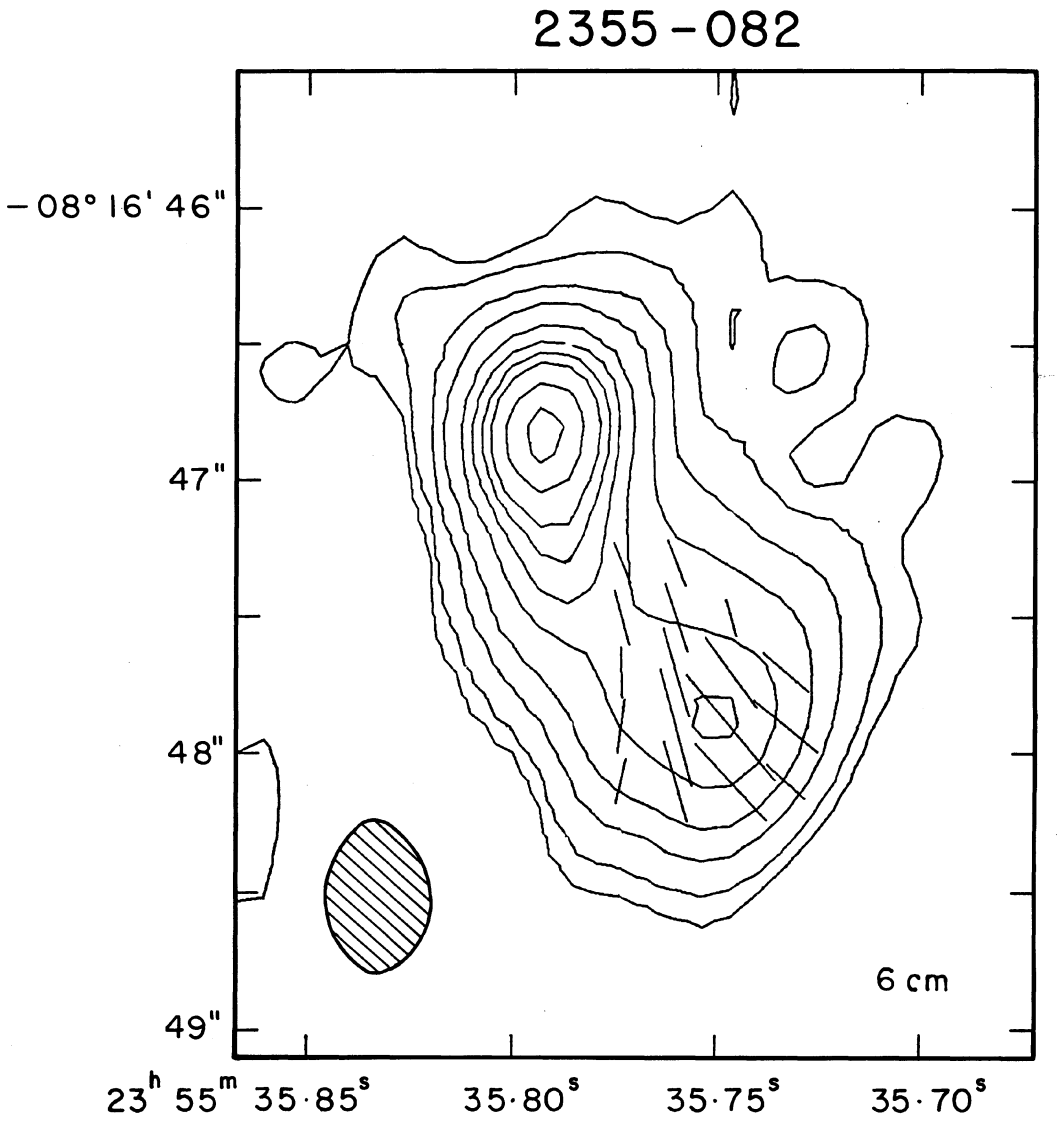

FIG. 1. (continued)

If the curvature changes sign, we call it wiggly. Note that these statements apply with our dynamic range of ~100. In particular, the structures called "bent" are not simply off-axis hot spots within a broader lobe structure. Within the dynamic range of the data, the whole of the detected structure is bent. By this criterion, we measure bending angles down to about 7°. Curvature of the bridge in our data is significant if it exceeds about 15°.

0007 + 106. Data originally reported in paper 1.

0017 + 257. Large curved triple structure. Core has weak small jet pointing (south) towards brighter lobe. HUO show a 20-cm map of this quasar. 20% of flux missing from our 20-cm map.

0041 + 119. Large triple structure. Weaker lobe is connected to the core by a wiggly bridge of emission. The strong lobe has complex structure, which is partly resolved at 6 cm.

0100 + 108. Double structure, both components having a steep spectrum. E component resolved at 6 cm. We measure the nearest optical object to be 8″ W, 14″ N of the published optical position. The radio sources lie about midway between these positions, ~8″ away from each. HUO report optical identification problems. Thus we cannot definitely classify the radio source.

0137 + 012. Complex curved structure in one lobe of a triple source. This object is fully discussed in a separate publication as a case of damped jet precession (Gower and Hutchings 1984). See also HUO. No strong correspondence with optical image intensity as published by WWG, but there is an optical extension or companion within 10% of the radio axis. The optical galaxy inner axis is parallel to the radio axis.

0241 + 622. This object was discussed in some detail in paper 1, in which radio and optical maps are shown. The radio extension is small scale, and both core and lobe are extended toward each other, but not along a straight line. The radio structure is at 90° to the optical long axis. The optical galaxy appears swept back from the radio extension.

0742 + 318. A radio map of this source is published by Neff (1982). It ~~is~~ a linear triple with a core jet pointing at one lobe. The geometry is very symmetrical. The optical structure is round and irregular. An optical jet or companion also lies at a small angle (10°) to the radio axis.

0846 + 100. The optical galaxy is irregular, with a nearby irregular object, and two others more distant. There is no clear correspondence between any of these and either the inner radio structure or the main large radio axis. The published (HB) position lies ~12″ NW of the radio core, but our remeasurement places it within 3″ of the radio core. ~15% of flux missing in our 20-cm map. The optical axis is within 10° of orthogonal to the radio.

0851 + 202. Unresolved in both radio and optical data.

0952 + 097. Compact triple source. SE lobe has sideways structure and low-intensity cavity towards the core source. ~45% of flux missing in our 20-cm data, indicating the presence of large-scale structure. HUO show a 20-cm map indicating extended emission around all three components.

0957 + 227. No radio source at the optical core. The optical object and close companion appear to lie in a region of low radio emission. The optical galaxy has no clear axis, but its inner isophotes are at 75 ± 10° to the radio axis. The axis of the optical interaction is at 60° to the radio extension. The radio structure of the NE component appears confined in the NW. Hintzen and Owen (1981) have published a 20-cm VLA snapshot. They also find an optical position (plotted) different from that published by HB. ~10% of flux missing in our 20-cm map.

1004 + 130. Very large and weak lobes. Our map is poor, probably confused, but the quasar core is clearly visible at both wavelengths. Large-scale structure published by Miley and Hartsuijker (1978).

1011 − 282. The optical position is at the SE (flat-spectrum) source. A faint extended southern lobe is seen at $10^h 11^m 15.1^s$ − 28°17′12″. The optical axis is at 10° ± 15% to the radio. An optical filament extends in the direction of the radio-intensity ridge to the NW. The northern lobe peak lies in an area free of optical emission.

1020 − 103. The radio source is resolved into two components, 1.5″ apart. The HB position is 3″ from the bright and 2″ from the faint radio sources. Our remeasurement of the optical position lies within 3″ of the bright source. Thus, while we can not say much about the exact position of the optical object, there is no reason to suppose it is not the correct object. The optical galaxy is regular and slightly elliptical, with long axis within 10° of the radio.

1028 + 313. Extended emission to the N is curved and extends into the core. Very weak Southern lobe.

1203 + 011. Radio source is just resolved (~0.2″ north-south) and the HB position is 30″ away. Our measured optical position is 7″ ± 5″ away, at $12^h03^m14.4^s$, 01° 10′ 31″. The optical source is unresolved, but has a faint (companion?) galaxy N of E.

1217 + 023. Large source with bent jets (Neff and Brown 1984). They show large-scale structure. Our data show only unresolved core and jet high points (hot spots).

1223 + 252. Very weak core source. Lobes have complex structure.

1243 − 072. See also Perley (1981). Optical long axis at 30 ± 10° to radio axis.

1254 − 333. Radio source has no core component, and edge-brightened lobes. The optical red image axis lies at 28 ± 10° to the radio. A blue optical extension to the SW points at the fainter radio lobe. A halo in red light trails to the NW. The radio data on their own indicate wiggling in the ridge line between the lobes. The lowest contour may be unreliable, and the high-frequency striations in the intensity an artifact of the analysis.

1302 − 102. This quasar galaxy is optically resolved in the red, but not in the blue. The bright radio cores lie on the optical QSO. The radio structure is small and curved ("banana" shape of Gower *et al.* 1982?). Optical data show no significant structure except in large outer halos, somewhat different in red and blue light, but extended E-W (at ~90° to the radio structure).

1400 + 162. This source has been discussed by Hintzen and Owen (1981), and optical data by Weistrop *et al.* (1983). The HB position lies ~15″ E of the radio core, but our remeasurement places it 5″ ± 5″ W of the core. Hintzen and Owen (1981) place it on the radio core. The radio structure is very complex, being bent overall, and with an inner curved jet seen at 6 cm. There is some optical emission to the SE, close to the inner radio jet blobs. There are two nearby galaxies with no associated radio emission. ~10% of flux missing in 20-cm map. The optical galaxy is elongated roughly along the radio axis.

1525 + 227. The radio source is small and double. The optical QSO coincides with the northern source. The southern radio component coincides with a faint optical object 5″ to the south of the QSO. The core source has different exten-

sions at each radio wavelength, and the optical QSO has structure to the NW which may be related.

1545 + 210. In this core-weak source, the hot spots and core are well aligned. The optical nucleus dominates in imaging data.

1635 + 119. The radio core source is unresolved. There are two other sources at $16^h35^m27.0^s$, 11°54.6′; $16^h35^m40.0^s$, 11°53.7′. Preliminary analysis of lower C-configuration data show the closer one to be a hot spot in a lobe to the south of the QSO. The optical long axis (Hutchings *et al.* 1984b) is at 70° to the radio axis.

1721 + 343. Barthel (1983) reports VLBI core structure. Large-scale structure published by Jagers *et al.* (1982).

1725 + 044. The optical QSO is in a crowded field, extended at ~90° to the radio axis. See also Perley (1981).

1739 + 184. Large source probably unreliable in A configuration map. (~40% flux missing). See also HUO. Their optical position (shown) differs from HB. The lobes are both extended in directions not passing through the core, with curvature.

2135 − 147. The radio source has two widely spaced large lobes, not detectably connected with the unresolved core. The optical QSO is a complex group of three interacting objects within a common halo. The group axis is aligned roughly with the radio axis, but the scale of the radio structure is ten times larger. Large-scale map published by Miley and Hartsuijker (1978). ~50% of the flux is missing from our 20-cm map.

2141 + 175. The radio source is unresolved. The optical QSO is very elongated at low light levels (see Hutchings *et al.* 1984).

2201 + 315. Optical QSO lies at radio core. Source has curved bridging luminosity between the core and lobes. Neff (1982) suggests a jet with changing orientation. The whole structure is bent at a small angle. Optical QSO has a halo which trails in the direction (NW) of the radio-source curvature. Outer optical isophotes are at 80 ± 10° to the radio axis. Optical companion has no radio emission. ~50% of flux missing in our 20-cm map.

2217 + 08. NE radio source is curved with jet pointing to SW (brighter) lobe. See Harris *et al.* (1983) for radio details. Optical QSO just resolved, with no significant structure (Hutchings *et al.* 1984).

2217 + 08. SW a triple source with a core jet to the W (Harris *et al.* 1983). Optical QSO has outer extensions at 90° to core jet direction, 60° to radio-structure bisector (Hutchings *et al.* 1984).

2247 + 140. See paper 1. Small radio extension at 80° to optical axis.

2305 + 187. See Gower *et al.* (1982) and Gower and Hutchings (1982) for full discussion. 20-cm map by HUO. Complex radio structure with axis at 60° to optical (Hutchings and Campbell 1983). NE optical extension coincides with faint radio emission.

2328 + 167. Not clear which, if either, component is the core.

2331 − 240. Radio source unresolved. Optical QSO amorphous and symmetrical, with possible blue bar.

2355 − 082. 20-cm map just resolved. Published (HB) position lies 9″ E of the radio source. Our remeasurement moves the position W by 17″ ± 8″. Thus, while uncertain, the optical position is compatible with the radio.

IV. RADIO PROPERTIES

Table III shows a summary of the principal radio properties of the sample, and Figs. 2 and 3 show the distributions of some of them. It has been remarked (e.g., Owen and Puschell 1983; Wilkinson 1983; HUO; Neff 1982) that quasars frequently have well-defined jets in their radio structure. In our sample, we find that over 50% have a bridge of connecting luminosity between the core and one or more outer lobes, at > 1% of the peak flux level. Of these, about 60% show bends or wiggles in the bridge, aside from any curvature due to the overall bending of the whole structure. About 40% have a jet or just-resolved structure connected to the core. As mentioned earlier, we do not find it useful at this stage to classify these structures in a way that implies a physical interpretation, and so do not discuss which of these conform to various definitions of a large-scale jet. Core luminosities range over three orders of magnitude, and source sizes over at least two orders of magnitude, before becoming too small to resolve. There is no correlation between the two quantities for the resolved sources, although there are not many objects of both 1–50 kpc size and low core luminosity. The distribution of core luminosities between different radio morphological types is shown in Fig. 2. Note that the lobe-dominated triples (shaded) are those with intrinsically weak cores, rather than

TABLE III. Summary of radio morphology.

Property	Whole Sample		Optically Imaged Sample	
Number	40(37)		24(23)	
Point Source	7	18%	5	21%
Point + 1 Lobe (CL)	8	20%	6	25%
Triple (T)	22	55%	11	46%
2 Lobes only (D)	3	8%	2	8%
Core structure	17	43%	12	48%
Bridge	22	55%	13	54%
Bent Source	11	28%	6	25%
Curved Bridge	13	32%	7	29%

Numbers in parentheses refer to objects with our own data only.

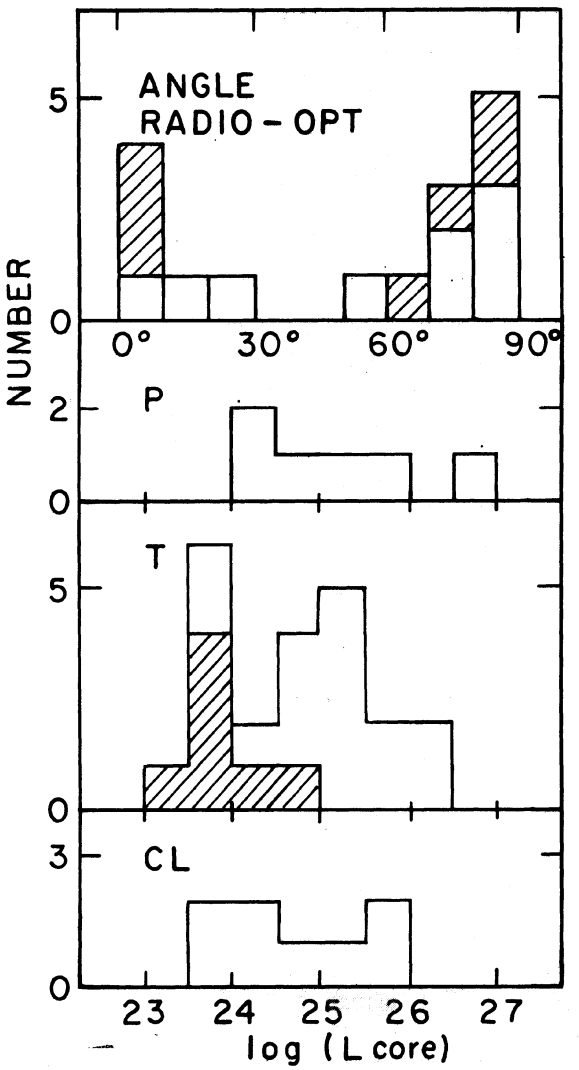

FIG. 2. Upper: histogram of angles between optical and radio long axes ($\pm$ 10°). Shaded values are less certain (see the text). Note clustering near zero and 90° values. Lower: distributions of radio core luminosity for unresolved (P), triple (T), and core plus single-lobe (CL) structures. Hatched areas indicate sources with core point fluxes weaker than the lobe peaks.

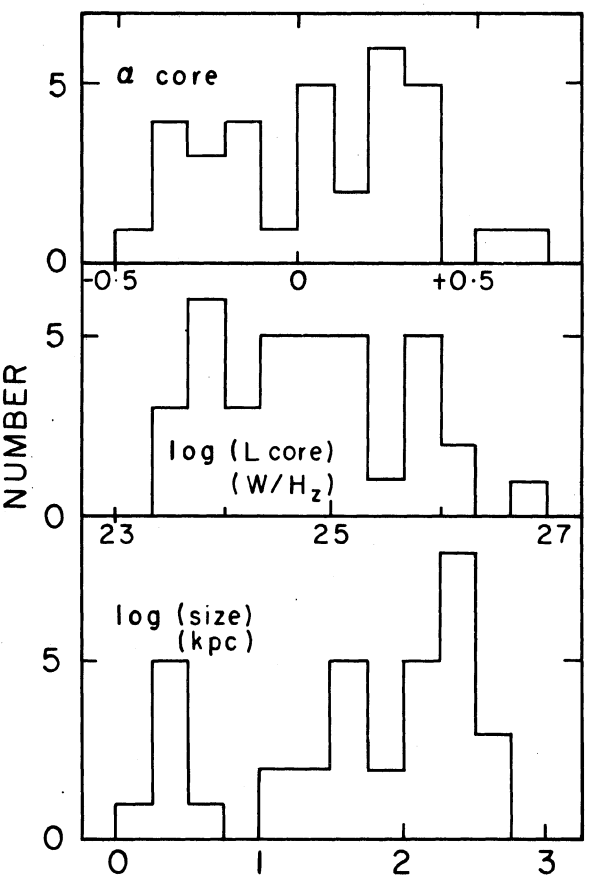

FIG. 3. Histograms of core spectral indices (negative = steep), core luminosities in W/Hz at 6 cm, and radio structure size in kpc, for the whole sample.

intrinsically strong lobes. This is consistent with the idea that the cores may fade significantly before the lobes. Note that two (possibly three) objects have no detectable core luminosity. The core luminosity is not correlated with its spectral index. Of the triple sources, about one-third have the core source weaker than the lobes.

The median size of the resolved sources is 53 kpc, in very close agreement with the value derived by Neff and Brown (1984) for a sample of low-redshift (< 0.9) quasars of comparable luminosity (our mean size is 130 kpc). Since their data also indicate a smaller size for high- luminosity quasars (< 10 kpc), there may be a size-luminosity trend (or upper envelope) at higher luminosities than we have in our sample.

For those sources sufficiently resolved to measure the flux of the unresolved core at both wavelengths, the spectral indices of the cores appear to range from about -0.5 to 0.7 with a flat distribution. The index does not appear to relate to other radio properties, but higher-resolution maps may show whether the range is due to the presence of steep spectrum structure . We note the absence of steeper spectrum cores with resolved structure of less than 50 kpc size.

Because of the variety of selection effects, source ages, and projection effects in this sample, together with a probable spread in intrinsic activity and velocity of moving material, potential correlations among the radio properties may be masked by a large scatter.

However, there are four well-resolved sources in this sample which show striking similarity in shape: 0017 + 257, 1400 + 162, 2217 + 08N, and 2201 + 315, in that all are appreciably curved, all have a jet-like structure close to the core which is only visible on one side, and all have brighter cores than average, both intrinsically and relative to the extended structure. Two main explanations for these curved structures are suggested:

(a) interaction of the quasar with the intergalactic medium (e.g., HUO);

(b) that these are quasars in which the jet axis is seen close to the line of sight, so that any intrinsic curvature [e.g., due to (a) above] appears amplified by projection effects, and, if the jets are even moderately relativistic, the luminosity of the core (and perhaps the jet) is Doppler boosted. Kapahi and Saikia (1982) explore the correlation between the ratio of intensities of the central core and the extended structure for

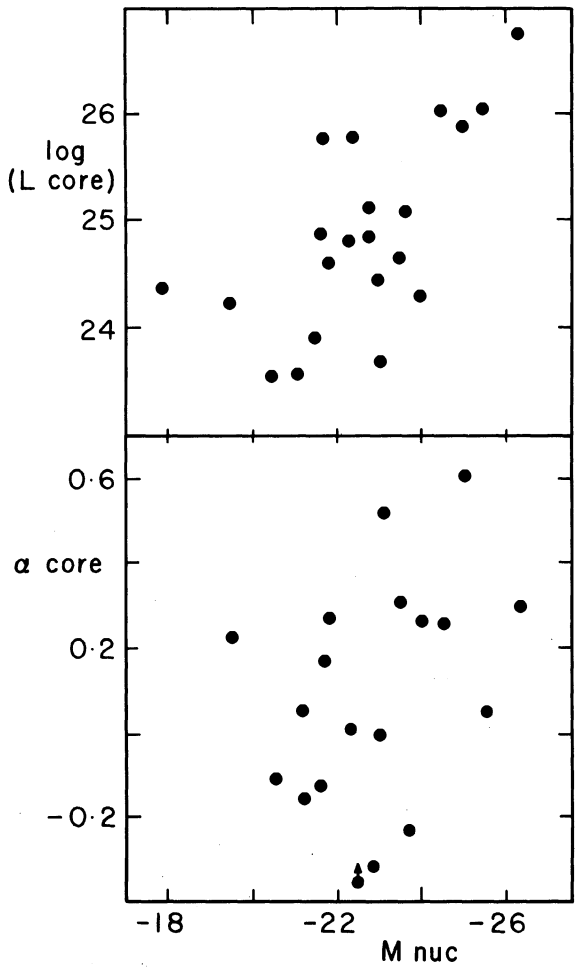

FIG. 4. Plot of core radio luminosity and core radio spectral index with optical nuclear luminosity for quasars in sample.

a large sample of quasars. Nine of the triple sources in our sample appear in their work, including 0017 + 257 and 1400 + 162, so that our sample is not independent of theirs, but we note that the properties of these four sources are in good agreement with their hypothesis. Furthermore, within this model, the extended structure surrounding 1400 + 162 finds a possible explanation as a double structure with extended outer lobes seen end-on, and therefore almost overlapping in projection. See also Browne and Orr (1982). Another possible source of this nature in our sample is 2305 + 187.

Before proceeding to the optical properties, we also summarize in Table III the radio properties in the optically studied subsample. Note that the properties of the optically studied objects are essentially the same as for the whole sample, lending confidence to the supposition that our samples are representative.

V. CORRELATION OF OPTICAL AND RADIO PROPERTIES

Optical data are given for most objects in HCC. We have looked for relationships between radio and optical properties in the principal data sets. Figures 4 and 5 show these relationships and also the principal optical properties of our sample, divided among the radio morphological types. With the small sample size we have, some apparent correlations may be spurious, but they indicate areas of interest for further study. Some of the obvious questions to consider are: (1) What is the difference between core-bright and lobe-dominated sources? (2) What is the difference between compact and large sources? (3) Is there evidence for beaming in both radio and optical radiation? (4) How are the radio and optical axes aligned? In answering these questions we must bear in mind the resolution limit in both data sets: we often do not know the optical galaxy type, and small-scale radio structure may be hidden in the data.

Many optical QSOs are found to have an apparently interacting small companion. Table IV shows a crude comparison of radio and optical morphological groups. All these comparisons are from our own (HCC) optical data only, particularly since other workers have not specifically commented on interaction detections. Most quantities are just what would be expected if the radio and optical properties were unrelated. However, the number of radio triples which are either optically interacting or members of optical groups are ~50% higher, suggesting possible connections. We note that of the 25 optical interaction detections in HCC, 13 are radio-selected objects and only three optically selected, which may be another sign of the first of these connections.

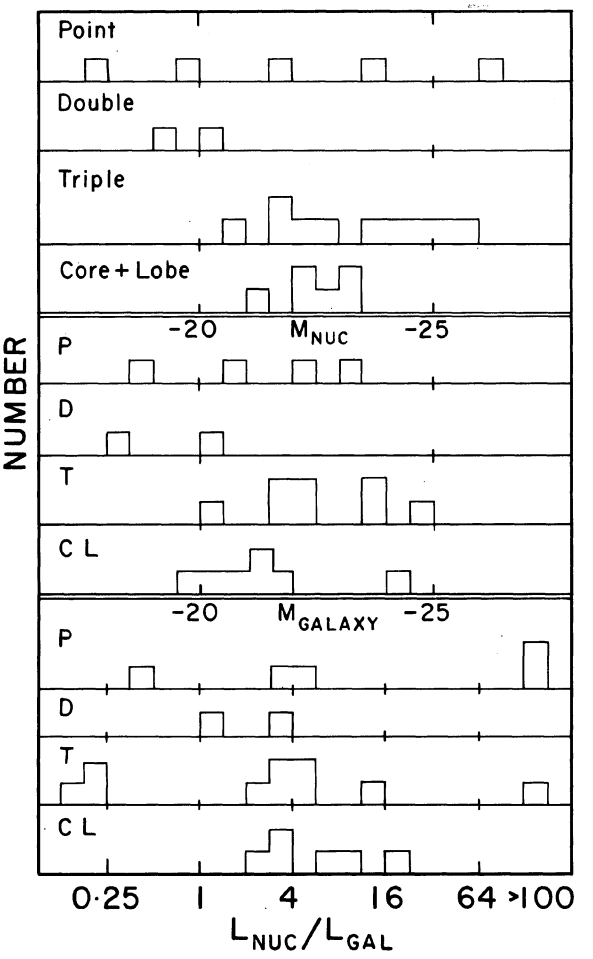

FIG. 5. Histograms of optical nuclear and host galaxy luminosities and their ratio for different types of radio structure.

TABLE IV. Morphology comparisons.

			Radio					
		Σ	6	2	10	6	11	6
			P	D	T	CL	>40	>100
	12	I	1	1	7	3	8	5
	9	G	2	0	6	1	5	3
Optical	3	H	0	1	2	0	3	0
	3	S	2	0	0	1	0	0
	2	F	2	0	0	0	0	0
	2	Ir	0	0	2	0	1	1

Optical I = Interacting
G = Group member
H = Halo
S = Spiral
F = Filament/Jet
Ir = Irregular contours

Radio P = Point (unresolved)
D = Double lobe only
T = Triple (core and lobes)
CL = Core and one lobe
>40 = larger than 40 Kpc
>100 = larger than 100 Kpc

Σ indicates totals of each kind. Note that all optical properties and last 2 radio are not mutually exclusive. First four radio are.

We might speculate that the interaction seen optically gives rise to the radio-triple (twin-jet) phenomenon. If so, the size of the radio structures compared with the separation of the two galaxies indicates roughly that the velocities of the radio-emitting material are at least an order of magnitude larger than the galaxy velocities, or 10^4 km s^{-1}. The results of HCC suggest that there are not many optically interacting QSOs which are not radio sources. The fraction of interactions which may give rise to QSO activity is compatible with the interaction scenario, as discussed by De Robertis (1983).

The most significant correlation is between the (log) radio core luminosity and the optical nuclear magnitude (Fig. 4: see also HCC). The correlation coefficient is 0.65 (> 99% probability). Note that this correlation is not a selection effect in flux-limited samples, since both radio and optical fluxes cover a range of > 50 at all redshifts. Since in HCC we find that host-galaxy magnitudes and nuclear magnitudes are related, there is also a correlation (slightly poorer) between log radio core luminosity and host-galaxy magnitude. Note that O'Dell *et al.* (1978) found a connection between total optical and radio flux in several sources.

The core spectral index also appears to vary with optical nuclear magnitude (Fig. 4; correlation coefficient 0.35, or 86% probability), with more luminous quasars having more inverted spectra. If this is a synchrotron self-absorption process, then it may be that it occurs more in more massive central engines.

Figure 2 shows the orientation comparisons. Of the 18 cases with optical mapping and radio structure, two have no clear optical axis, six have poorly defined optical axes (halos, possible rotation of isophotes, or possible faint companions), and three have bent or curved radio structure (see Sec. III for remarks and angles). Nine good comparisons are possible, with uncertainties $\pm$ 10° or less. Optical axes are defined by fitting ellipses to isophotes (HCC), where this orientation does not change over the outer isophotes by more than this uncertainty. The diagram distinguishes between good and less certain values, but there is, in any case, an apparent grouping near 90°, in line with the expectation that the radio-emitting material is ejected along the short axis of the galaxy. For the range of angles 45°–90°, our error estimates predict a mean measured value of 80° if the real inclination is always 90°, and a mean measured value of 67° if they are random. The actual value is 77°, suggesting a real grouping near 90°. There is also a grouping of less well-defined points near 0°. There is no correlation between radio emission and optical position of the interacting companion galaxy. Where optical halos and radio structure appear swept back by a moving medium, two cases indicate the same motion, and the three others have opposing directions, lying between 120° and 180°.

In our sample, triple sources have host galaxies with a large optical scale length (3 kpc mean) compared with doubles (1.2 kpc) and point sources (1.9 kpc) (HCC). If quasars are activated by galaxy interactions, we may expect them to look different either (a) by the exact nature of the event, (b) by the time since the event, or (c) by differences in our lines of sight to different objects. These apparent connections may relate to such differences.

In Table IV, the three objects with recognized spiral struc-

ture have small radio structure. However, the galaxy type is not uniquely determined for the large radio sources (see HCC).

Finally, we note in Fig. 5 some of the distributions of optical quantities in our sample, among the different radio-source structure types. These may be chance difference (either due to selection effects or small number statistics), or indications of real group characteristics. For instance, the optical ratio of nuclear to galaxy luminosity ($L_{\rm nuc}/L_{\rm gal}$) may indicate either optical beaming or the (isotropic) activity of the nucleus relative to the host galaxy. In our sample, single-lobe sources (CL) appear to have a small range in $L_{\rm nuc}/L_{\rm gal}$, and also to have a higher mean $L_{\rm nuc}/L_{\rm gal}$ ratio (8) than other groups (Fig. 5), thus consistent with both optical and radio beaming. See Kapahi and Saikia (1982) for further discussion on this question. The optical $L_{\rm nuc}/L_{\rm gal}$ ratio is not related to the radio core spectral index.

VI. DISCUSSION AND SUMMARY

We have made a comparison of optical and radio morphology of quasars. A number of interesting correlations are indicated, which need some confirmation, and whose interpretation is not immediately obvious. They relate as follows to the four questions noted in the previous section. (1) There may be a connection between triple radio sources and QSOs which are interacting or in close groups of galaxies (Table IV). [At the radio luminosities in our sample, they are large sources, but high-luminosity quasars may be smaller (Neff and Brown 1984)]. The suggestion is that lobes form soon after a quasar is powered up and remain luminous some time after the radio quasar begins to fade. Most of the bridges between core and lobes are wiggly, which implies that instabilities set in or the beams undergo a change in orientation in times less than the age of the emitting material (often thought to be $\lesssim 10^7$ yr). These latter cases, we suggest, are seen when the encounter is very close (Wirth *et al.* 1982), or in some cases when a nuclear merger occurs (Gower *et al.* 1982). (2) Our sample can not answer the question as to the difference between compact and large radio sources, since we are unable to disentangle the effects of the large number of other parameters which may modify the apparent source size: e.g., luminosity, age, orientation, host-galaxy mass. (3) There are some sources consistent with beaming, but they are also consistent with unbeamed models. For instance, single-lobe sources have a small range and higher mean value of optical nuclear to galaxy luminosity than other radio types (Fig. 5). As such evidence always seems to be mixed, we suspect that some of the radio sources (or some part of all sources) are beamed and some are not. (4) Radio emission along the galaxy short axis appears to be the norm, but apparent alignment is also seen. It is not clear if the latter is optical emission from the radio beam, a real alignment with the galaxy plane, or a projection effect. The normal situation, as expected, seems to be that jets emerge normal to a galaxy disk.

Both the significance of these apparent correlations and their interpretation require further work with a larger sample of data.

Finally, for our data set, we summarize the other results or indications with the following points. We stress that these apply to our data set only, and the suggestions all need further investigation with a larger sample.

(1) About 25% of the low-redshift quasars have a bent radio structure, suggesting interaction with a surrounding medium, or nonaligned ejection directions (Table I).

(2) Radio core luminosity increases with optical nuclear luminosity (Fig. 4).

(3) Lobe-bright sources have intrinsically weaker core sources than core-bright sources (Fig. 2).

(4) The median resolved source size is 53 kpc, core luminosity $10^{24.9}$ W/Hz, core spectral index 0.1 (Fig. 3).

(5) The core spectral index appears more inverted for more luminous optical quasars (Fig. 4).

We thank the VLA staff for much help and advice; particularly Rick and Peggy Perley and Phillip Hicks. ACG acknowledges an AAS small research grant and an NSERC grant through the University of Victoria. We thank the following for discussion during the course of the work: P. Barthel, P. Hintzen, S. Neff, R. Sramek, and H. van der Laan. We acknowledge the useful and critical comments of a referee.

REFERENCES

Barthel, P. (1983). Private communication.
De Robertis, M. M. (1983). Preprint.
Gower, A. C., and Hutchings, J. B. (1982). Astrophys. J. Lett. **253**, L 1.
Gower, A. C., and Hutchings, J. B. (1984). Publ. Astron. Soc. Pac. **96**, 19.
Gower, A. C., Gregory, P. C., Hutchings, J. B., and Unruh, W. G. (1982). Astrophys. J. **262**, 478.
Harris, D. E., Dewdney, P. E., Costain, C. H., Butcher, L., and Willis, A. G. (1983). Astrophys. J. **270**, 39.
Hewitt, A., and Burbidge, G. R. (1980). Astrophys. J. Suppl. **43**, 57.
Hintzen, P., and Owen, F. N. (1981). Astron. J. **86**, 1577.
Hintzen, P., Ulvestad, J., and Owen, F. N. (1983). Astron. J. **88**, 709 (HUO).
Hutchings, J. B., Campbell, B., Crampton, D., Gower, A. C., and Morris, S. C. (1982). Astrophys. J. **262**, 48 (paper 1).
Hutchings, J. B., Crampton, D., and Campbell, B. (1984). Astrophys. J. **280**, 41. (HCC).
Hutchings, J. B., Crampton, D., Campbell, B., Duncan, D., and Glendenning, B. (1984). Astrophys. J. Suppl. **55**, 319.
Hutchings, J. B., and Campbell, B. (1983). Nature **303**, 584.
Jagers *et al.* (1980). Astron. Astrophys. **105**, 279.
Kapahi, V. K., and Saikia, D. J. (1982). J. Astrophys. Astron. **3**, 465.
Miley, G. K., and Hartsuijker, A. P. (1978). Astron. Astrophys. Suppl. **34**, 129.
Miley, G. K., and Miller, J. S. (1979). Astrophys. J. Suppl. **34**, 129.
Miley, G. K., and Miller, J. S. (1979). Astrophys. J. **228**, L55.
Neff, S. G. (1982). Thesis, University of Virginia.
Neff, S. G., and Brown, R. (1984). Astron. J. **89**, 195.
O'Dell *et al.* (1978). Astrophys. J. **224**, 22.
Orr, M. J. L., and Browne, I. W. A. (1982). Mon. Not. R. Astron. Soc. **200**, 1067.
Owen, F. N., and Puschell, J. J. (1983). Preprint.
Weistrop, D., Schaffer, D. B., Reitsama, H. J., and Smith, B. A. (1983). Astrophys. J. **271**, 471.
Wilkinson, P. (1983). *IAU Symposium 110* (Reidel, Dordrecht). (in press).
Wirth, A., Smarr, L., and Gallagher, J. S. (1982). Astron. J. **87**, 602.
Wyckoff, S., Wehinger, P. A., and Gehren, T. (1981). Astrophys. J. **247**, 750 (WWG).